

Three-mode Gaussian states in quantum information with continuous variables

Gerardo Adesso^{1,2}, Alessio Serafini^{3,4} and Fabrizio Illuminati¹

¹Dipartimento di Fisica “E. R. Caianiello”, Università degli Studi di Salerno; CNR-Coherentia, Gruppo di Salerno; and INFN Sezione di Napoli-Gruppo Collegato di Salerno; Via S. Allende, 84081 Baronissi (SA), Italy

²Centre for Quantum Computation, DAMTP, Centre for Mathematical Sciences, University of Cambridge, Wilberforce Road, Cambridge CB3 0WA, United Kingdom

³Institute for Mathematical Sciences, Imperial College London, 53 Prince’s Gate, SW7 2PE, United Kingdom; and QOLS, The Blackett Laboratory, Imperial College London, Prince Consort Road, SW7 2BW, United Kingdom

⁴Department of Physics & Astronomy, University College London, Gower Street, London WC1E 6BT, United Kingdom

E-mail: gerardo@sa.infn.it, serale@imperial.ac.uk, illuminati@sa.infn.it

Abstract. The structural aspects of tripartite entanglement in three-mode Gaussian states of continuous variable systems have been studied in [Adesso G, Serafini A and Illuminati F 2006 *Phys. Rev. A* **73** 032345]. Here we focus our attention on the usefulness of such states in the context of realistic processing of continuous-variable quantum information. We introduce and discuss in detail several examples of pure and mixed three-mode states that stand out for their informational and/or entanglement properties. We then describe practical schemes to engineer such states with linear optics. In particular, we introduce a simple procedure – based on passive optical elements – to produce pure three-mode Gaussian states with *arbitrary* entanglement structure (upon availability of an initial single-mode squeezed state). We analyze in detail the properties of distributed entanglement, showing that the promiscuity of entanglement sharing is a feature peculiar to symmetric Gaussian states that survives even in the presence of significant degrees of mixedness and decoherence. Next, we discuss the suitability of the considered tripartite entangled states to the implementation of quantum information and communication protocols with continuous variables. This will lead to a feasible experimental proposal to test the promiscuous sharing of continuous-variable entanglement, in terms of the optimal fidelity of teleportation networks with Gaussian resources. As a byproduct, optimal resource states for various communication protocols (among which asymmetric telecloning) will be exactly determined.

Contents

1	Introduction	3
2	Three-mode Gaussian states: structural properties	3
2.1	Separability properties	4
2.2	Standard forms	5
3	Tripartite continuous variable entanglement	7
3.1	Entanglement sharing and monogamy constraints	7
3.2	Residual tripartite entanglement (<i>arravogliamento</i>)	8

4 Relevant families of three-mode Gaussian states: Entanglement properties and quantum state engineering	8
4.1 The ‘allotment’ box for the production of arbitrary three-mode pure states	8
4.2 Continuous-variable GHZ/W states	11
4.3 T states with zero reduced bipartite entanglement	13
4.4 Promiscuous entanglement sharing: The power of symmetric resources	14
4.5 Noisy GHZ/W states: The effect of mixedness	15
4.6 Basset-hound states: A ‘traditional’ sharing of entanglement	18
5 Application: Multiparty quantum teleportation with continuous variables	19
6 Teleportation networks with fully symmetric resources	20
6.1 Equivalence between multipartite entanglement and optimal fidelity	21
6.2 Testing the promiscuous sharing of tripartite entanglement	23
6.3 Degradation of teleportation efficiency under quantum noise	25
7 $1 \rightarrow 2$ telecloning with bisymmetric and nonsymmetric resources	27
7.1 Symmetric telecloning	27
7.2 Asymmetric telecloning	30
8 Conclusions	32
Acknowledgments	33
References	33

1. Introduction

The study of multipartite entanglement in Gaussian states of continuous variable (CV) systems has lately received much attention, both in view of their interest as a theoretical testground and because of their versatility towards the effective implementation of communication protocols. Nevertheless, a complete understanding of the general features of multipartite quantum correlations and of their (often controversial) operational interpretation still appears to be far from accomplished.

For the basic instance of three-mode Gaussian states, a qualitative classification of multipartite entanglement has been introduced [1], while more recently a consistent way to quantify such a multipartite entanglement has been presented, with the definition of the “residual (Gaussian) contangle” [2]. However, even for three-mode Gaussian states, many important aspects related to the complex sharing structure of quantum correlations between the three parties wait for further inspection and clarification.

The purpose of this paper is twofold. Firstly, it presents practical strategies to engineer three-mode Gaussian entangled resources, which may have a remarkable experimental impact towards the practical realization of optimal resources for specific multipartite communication tasks. Secondly, it aims at providing the residual contangle and its properties with an operational interpretation by addressing its relationship with the figures of merits of optimized communication protocols (teleportation networks and telecloning). As we will see, these two objectives are intimately intertwined, as they both concern the characterization of the structure of multipartite entanglement and of its sharing properties.

The article opens with a review of the basic properties of three-mode Gaussian states (Sec. 2) and of the known mathematical properties of their entanglement, to proceed with the definition of the residual Gaussian contangle (Sec. 3). We then provide a general recipe to build pure three-mode Gaussian states with any arbitrary entanglement structure, and presents an extensive classification of pure and noisy three-mode Gaussian states into several families, characterized by different symmetry and entanglement properties (Sec. 4). Sec. 5 introduces the second part of the paper, devoted to communication protocols: we address optimal fidelities of three-party teleportation networks (Sec. 6) and symmetric and asymmetric telecloning (Sec. 7), determining various instances of three-mode states acting as optimal resources for such protocols. Sec. 8 concludes the paper, finalizing the line of work undertaken in Ref. [2] and completed in the present article.

2. Three-mode Gaussian states: structural properties

We consider a continuous variable (CV) system consisting of N bosonic modes, associated to an infinite-dimensional Hilbert space \mathcal{H} and described by the vector $\hat{X} = \{\hat{x}_1, \hat{p}_1, \dots, \hat{x}_N, \hat{p}_N\}$ of the field quadrature operators, whose canonical commutation relations can be expressed in matrix form: $[\hat{X}_i, \hat{X}_j] = 2i\Omega_{ij}$, with the symplectic form $\Omega = \bigoplus_{i=1}^n \omega$ and $\omega = \delta_{ij-1} - \delta_{ij+1}$, $i, j = 1, 2$.

Quantum states of paramount importance in CV systems are the so-called Gaussian states, *i.e.* states with Gaussian characteristic functions and quasi-probability distributions [3, 4, 5]. The interest in this special class of states (which includes vacua, coherent, squeezed, thermal, and squeezed-thermal states of the electromagnetic field) stems from the feasibility to produce and control them with linear optical elements, and from the increasing number of efficient proposals and successful experimental implementations of CV quantum information and communication processes involving multimode Gaussian states. For a review of the basic properties of Gaussian states, see *e.g.* Ref. [2], which is focused on three-mode states

and contains an extensive general introduction to phase-space formalism and symplectic operations (making use of the same notation adopted here). In this section, we limit ourselves to define the relevant notation and recall some useful results.

Neglecting first moments (which can be arbitrarily adjusted by local unitaries), one can completely characterize a Gaussian state by the real, symmetries covariance matrix (CM) σ , whose entries are $\sigma_{ij} = 1/2\langle\{\hat{X}_i, \hat{X}_j\}\rangle - \langle\hat{X}_i\rangle\langle\hat{X}_j\rangle$. Throughout the paper σ will be used indifferently to indicate the CM of a Gaussian state or the state itself. The CM σ must fulfill the Robertson-Schrödinger uncertainty relation $\sigma + i\Omega \geq 0$ [6].

For future convenience, let us write down the CM σ of a 3-mode Gaussian state in terms of two by two submatrices as

$$\sigma = \begin{pmatrix} \sigma_1 & \varepsilon_{12} & \varepsilon_{13} \\ \varepsilon_{12}^\top & \sigma_2 & \varepsilon_{23} \\ \varepsilon_{13}^\top & \varepsilon_{23}^\top & \sigma_3 \end{pmatrix}. \quad (1)$$

2.1. Separability properties

The positivity of the partially transposed CM $\tilde{\sigma}$ has been proven to be necessary and sufficient for the separability of $(1+N)$ -mode and bisymmetric $(M+N)$ -mode Gaussian states [7, 8, 9, 10], providing a clearcut qualitative characterization of the entanglement of such states. An ensuing computable measure of CV entanglement is the *logarithmic negativity* [11] $E_N \equiv \log_2 \|\tilde{\rho}\|_1$, where $\|\cdot\|_1$ denotes the trace norm, which constitutes an upper bound to the *distillable entanglement* of the state ρ . For Gaussian states, it can be computed in terms of the symplectic spectrum $\tilde{\nu}_i$ of the partially transposed CM $\tilde{\sigma}$ [2]:

$$E_N = \max \left\{ 0, -\sum_{i: \tilde{\nu}_i < 1} \log_2 \tilde{\nu}_i \right\}. \quad (2)$$

A complete *qualitative* characterization of the entanglement of three-mode Gaussian state has been obtained in [1], where five different cases have been identified:

- Class 1: states not separable under any bipartition of the modes ('fully inseparable states', possessing "genuine" tripartite entanglement).
- Class 2: states separable under only one bipartition ('one-mode biseparable states').
- Class 3: states separable only under two bipartitions out of three ('two-mode biseparable states').
- Class 4: states separable under all three bipartitions but impossible to write as a convex sum of pure, three-mode product states ('three-mode biseparable states').
- Class 5: states which can be written as a convex sum of pure, three-mode product states ('fully separable states').

Notice that classes 4 and 5 cannot be discriminated by partial transposition with respect to any of the three modes (which is positive for both classes): the entanglement of class-4 states is thus undistillable, and these states provide an instance of tripartite, bound entangled states [1].

Adopting a more practical-oriented viewpoint, let us recall that efficient criteria to detect multipartite entanglement from the knowledge of the second moments (*i.e.* of the CM's elements) have been developed [12]. Let $\hat{u} \equiv \sum_{j=1}^3 h_j \hat{x}_j$ and $\hat{v} \equiv \sum_{j=1}^3 g_j \hat{p}_j$ for some real coefficients $\{g_j, h_j\}$ and let $\langle(\Delta\hat{o})\rangle_\rho$ be the squared variance of the generic operator \hat{o} : $\langle(\Delta\hat{o})\rangle_\rho \equiv \text{Tr}[\rho(\hat{o} - \text{Tr}[\rho]\hat{o})^2]$. A *sufficient* condition to detect the presence of entanglement in a three-mode state ρ with respect to, say, the bipartition 1|23 is then given by

$$\langle(\Delta\hat{u})^2\rangle_\rho + \langle(\Delta\hat{v})^2\rangle_\rho < (|h_1g_1| + |h_2g_2 + h_3g_3|)/2. \quad (3)$$

By choosing $h_1 = g_1 = 1$ and $g_2 = g_3 = -h_2 = -h_3 = 1/\sqrt{2}$ and by considering the permutations of the indexes in the previous equation, such a condition can be turned into a single sufficient condition to detect genuinely multipartite entanglement (*i.e.* to detect ‘class 1’ states), given by

$$\langle \{\Delta[\hat{x}_1 - (x_2 + x_3)/\sqrt{2}]\} \rangle_\varrho + \langle \{\Delta[\hat{p}_1 + (p_2 + p_3)/\sqrt{2}]\} \rangle_\varrho < 1/2. \quad (4)$$

Notice that these combinations of quadratures are chosen such that their commutator vanishes, thus allowing arbitrarily large violation of the previous inequality (see Ref. [12]).

Let us finally remark that another effective way of testing the presence of bipartite and/or genuine tripartite entanglement in Gaussian states is through *entanglement witnesses*, based on linear and nonlinear functionals of the CM [13].

2.2. Standard forms

As demonstrated in Ref. [2], the three local symplectic invariants $\text{Det } \boldsymbol{\sigma}_1$, $\text{Det } \boldsymbol{\sigma}_2$ and $\text{Det } \boldsymbol{\sigma}_3$ (strictly related to the local mixednesses of the state [14]) fully determine the entanglement of any possible bipartition of a pure three-mode Gaussian state with CM $\boldsymbol{\sigma}$, and also the genuine tripartite entanglement contained in the state [15]. Moreover, defining $a_j \equiv \sqrt{\text{Det } \boldsymbol{\sigma}_j}$ for $j = 1, \dots, 3$ one has that the three single-mode mixednesses are constrained by the following ‘triangle’ entropic inequality (see [2] for a detailed proof)

$$|a_i - a_j| + 1 \leq a_k \leq a_i + a_j - 1. \quad (5)$$

Remarkably, Inequality (5) (together with the conditions $a_l \geq 0 \ \forall l$) fully characterizes the local symplectic eigenvalues of the CM of three-mode pure Gaussian states, thus providing a complete characterization of the entanglement of such states. In fact, the CM of Eq. (1) can be put in a *standard form* completely parametrized by the three local mixednesses, with $\boldsymbol{\sigma}_i = \text{diag}\{a_i, a_i\}$ and the blocks $\boldsymbol{\varepsilon}_{ij}$ diagonal as well, with elements only functions of the $\{a_i\}$ ’s [2].

Before proceeding, let us define classes of states endowed with symmetries under mode exchange, which we will refer to as ‘bisymmetric’ and ‘fully symmetric’ states. Specializing to a three-mode instance, *bisymmetric* states are Gaussian states invariant under the exchange of two given modes (say 2 and 3) [10, 16], such that their CM $\boldsymbol{\sigma}_{\text{bis}}$ has the form

$$\boldsymbol{\sigma}_{\text{bis}} = \begin{pmatrix} \alpha & \boldsymbol{\varepsilon} & \boldsymbol{\varepsilon} \\ \boldsymbol{\varepsilon}^T & \beta & \boldsymbol{\zeta} \\ \boldsymbol{\varepsilon}^T & \boldsymbol{\zeta}^T & \beta \end{pmatrix}. \quad (6)$$

Bisymmetric Gaussian states possess relevant entanglement properties: as already mentioned, the positivity of the partial transposition is a necessary and sufficient condition for these states to be separable (for any total number of modes). This is due to the fact that their entanglement can be concentrated into two modes by local symplectic operations. Suppose that Alice owns mode 1 while Bob owns the block 2 – 3 of a bisymmetric state, then Bob can apply a local unitary (symplectic in phase space) operation on his block, so that the whole original three-mode entanglement will be concentrated between the single mode owned by Alice, and only one of the two modes owned by Bob. Because of the symmetry, the local symplectic transformation responsible for entanglement concentration is typically (if the CM is in ‘standard form’, with the single-mode blocks in their Williamson diagonal form) a simple beam splitter. In general, it may include a combination of beam splitters, phase shifters and squeezers, *i.e.* passive and active operations which are currently in the toolbox of experimental quantum optics. The power of this process is in its complete reversibility. Namely, suppose that Bob needs to reconstruct the original state, with his two modes in an entangled state with

Three-mode Gaussian states

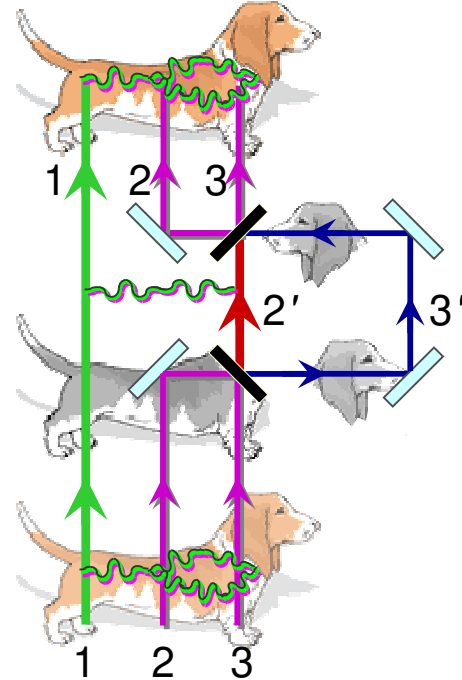


Figure 1. IF YOU CUT THE HEAD OF A BASSET HOUND, IT WILL GROW AGAIN [17]. Graphical depiction of the process of unitary localization (concentration) and delocalization (distribution) of entanglement in three-mode bisymmetric Gaussian states [10] (or “basset-hound” states), described in the text. Initially, mode 1 is entangled (entanglement is depicted as a waving string) with both modes 2 and 3. It exists a local (with respect to the $1|(23)$ bipartition) symplectic operation, realized e.g. via a beam splitter (denoted by a black thick dash) such that all the entanglement is concentrated between mode 1 and the transformed mode $2'$, while the other transformed mode $3'$ decouples from the rest of the system (*unitary localization*). Therefore, the head of the basset hound (mode $3'$) has been cut off. However, being realized through a symplectic operation (*i.e.* unitary on the density matrix), the process is reversible: operating on modes $2'$ and $3'$ with the inverse symplectic transformation, yields the original modes 2 and 3 entangled again with mode 1, without any loss of quantum correlations (*unitary delocalization*): the head of the basset hound is back again.

the mode shared by Alice. He can then simply let his transformed two modes (one of which was uncorrelated from the rest) interfere at the reversed beam splitter (in general, the inverse symplectic operation), so that the original state is recovered. The entire procedure, technically known as “unitary localization and delocalization” of entanglement [10], may be referred to as “cut-off and regrowth of the head of a basset hound”, as depicted in Fig. 1. In our example, the basset hound pictorially represents a three-mode state. However, as the breed of the dog suggests, the unitary localizability is a property that extends to all $1 \times N$ [16] and $M \times N$ [10] bisymmetric Gaussian states, enabling Alice and Bob (when owing multiple modes) to realize by purely local control a perfect and reversible two-mode/multimode entanglement switch by means of linear optical devices.

As a special case, *fully symmetric* Gaussian states are invariant under the exchange of any pair of modes, with a CM σ_s given by

$$\sigma_s = \begin{pmatrix} \alpha & \varepsilon & \varepsilon \\ \varepsilon^T & \alpha & \varepsilon \\ \varepsilon^T & \varepsilon^T & \alpha \end{pmatrix}. \quad (7)$$

Obviously, fully symmetric states are bisymmetric under any bipartition of the modes; this, in brief, means that any conceivable three-mode, bipartite entanglement is locally equivalent to the minimal two-mode, bipartite entanglement. Pictorially, this special type of basset-hound state resembles a *Cerberus* state, in which any one of the three heads can be cut and can be reversibly regrown. It is worth stressing that fully symmetric Gaussian states include nearly all the states of tripartite CV systems currently produced in the laboratory by quantum optical means [18, 19]; we will discuss their usefulness as resources for quantum communication protocols with continuous variables in Sec. 6.

3. Tripartite continuous variable entanglement

3.1. Entanglement sharing and monogamy constraints

Recently, an analysis of the sharing properties of multipartite entanglement in Gaussian states of CV systems has lead to the proof that CV entanglement obeys a monogamy inequality [15, 20], analogous to the Coffman-Kundu-Wootters (CKW) monogamy constraint in three- and many-qubit systems [21, 22]. This result, holding in general N -mode Gaussian states [20], will be exploited here in the case $N = 3$. Namely, the monogamy inequality

$$E^{i|(jk)} - E^{i|j} - E^{i|k} \geq 0, \quad (8)$$

first established for three-qubit systems by Coffman, Kundu and Wootters [21], holds true for generic (pure or mixed) three-mode Gaussian states [15, 2]. In Ineq. (8), i, j, k denote the three elementary parties (modes in a CV system), and E refers to a bipartite entanglement monotone known as the *contangle* [15].

The contangle E_τ of a state ρ is formally defined as the convex roof of the squared logarithmic negativity[‡]:

$$E_\tau(\rho) \equiv \inf_{\{p_i, \psi_i\}} \sum_i p_i E_\tau(\psi_i), \quad \text{with } E_\tau(\psi_i) = \log_2^2(\|\tilde{\psi}_i\|) \quad (9)$$

where the infimum is taken over *all* convex decompositions of ρ in terms of pure states $\{|\psi_i\rangle\}$ and “ \sim ” denotes partial transposition. Let us remark that the contangle of a pure $(1+N)$ -mode Gaussian state $|\psi\rangle$ with CM σ_p is easily obtained as $E_\tau = \text{arcsinh}^2(\sqrt{1 - \mu_1^2}/\mu_1)$, where $\mu_1 = 1/\sqrt{\text{Det } \sigma_1}$ is the local purity of the reduced state of mode 1.

Notice that any multimode mixed Gaussian state with CM σ , admits a decomposition in terms of pure Gaussian states only. The infimum of the average contangle, taken over all pure Gaussian state decompositions, defines the *Gaussian contangle* G_τ . It can be expressed in terms of CMs as

$$G_\tau(\sigma) = \inf_{\sigma^p \leq \sigma} E_\tau(\sigma^p), \quad (10)$$

[‡] Being the negativity a convex function of the logarithmic negativity (specifically, an exponential), the validity of a monogamy constraint for three-mode Gaussian states using as an entanglement measure the convex-roof extended squared negativity (also known as Gaussian tangle [20]), is implied by the proof of the corresponding CKW inequality for the contangle [15].

where the infimum runs over all pure Gaussian states with CM $\sigma^p \leq \sigma$. Let us remark that, if σ_s denotes a mixed symmetric (1×1) -mode Gaussian state, then the decomposition of σ_s in terms of an ensemble of pure Gaussian states is the optimal one [23] (it is currently an open question whether this is true for all Gaussian states [24]), which means that the Gaussian contangle coincides with the true one. Moreover, the optimal pure-state CM σ_s^p minimizing $G_\tau(\sigma_s)$ in Eq. (10) is characterized by having $\tilde{\nu}_-(\tilde{\sigma}_s^p) = \tilde{\nu}_-(\tilde{\sigma}_s)$ [23, 25]. The fact that the smallest symplectic eigenvalue is the same for both partially transposed CMs entails for symmetric two-mode Gaussian states that

$$E_\tau(\sigma_s) = G_\tau(\sigma_s) = [\max\{0, -\log_2 \tilde{\nu}_-(\sigma_s)\}]^2. \quad (11)$$

Of course $E_\tau = G_\tau$ also in all *pure* Gaussian states of $1 \times N$ bipartitions.

3.2. Residual tripartite entanglement (arravogliament)

From the sharing constraint, the minimum *residual contangle* [15, 26] emerges as a quantifier of genuine tripartite entanglement:

$$E_\tau^{i|j|k} \equiv \min_{(i,j,k)} \left[E_\tau^{i|(jk)} - E_\tau^{i|j} - E_\tau^{i|k} \right], \quad (12)$$

where (i, j, k) denotes all the permutations of the three mode indexes. Adopting an analogous definition, the minimum residual Gaussian contangle G_τ^{res} , compactly referred to as *arravogliament* (or “arravojament”) [15, 2], reads

$$G_\tau^{res} \equiv G_\tau^{i|j|k} \equiv \min_{(i,j,k)} \left[G_\tau^{i|(jk)} - G_\tau^{i|j} - G_\tau^{i|k} \right]. \quad (13)$$

One has that

$$(G_\tau^{i|(jk)} - G_\tau^{i|k}) - (G_\tau^{j|(ik)} - G_\tau^{j|k}) \geq 0 \quad \text{if and only if} \quad a_i \geq a_j, \quad (14)$$

and therefore the absolute minimum in Eq. (13) is attained by the decomposition realized with respect to the reference mode l of smallest local mixedness a_l . Let us remark that for pure three-mode Gaussian states the arravogliament is an entanglement monotone under tripartite GLOCC [15]

4. Relevant families of three-mode Gaussian states: Entanglement properties and quantum state engineering

In this section we provide the reader with a systematic analysis of several classes of three-mode Gaussian states, characterized by peculiar structural and/or entanglement properties. We shall focus on bipartite and tripartite entanglement of these classes, and outline schemes for their state engineering with current optical technology.

4.1. The “allotment” box for the production of arbitrary three-mode pure states

The computation of the tripartite entanglement, quantified by the residual Gaussian contangle of Eq. (13) (arravogliament), in generic *pure* three-mode Gaussian states has been presented in full detail in Ref. [2]. Here we investigate how to engineer these states, allowing for any possible entanglement structure.

A viable scheme to produce all pure three-mode Gaussian states, as inspired by Euler decomposition [27], would combine three independent squeezed modes (with in principle all different squeezing factors) into any conceivable combination of orthogonal (energy preserving) symplectic operations (essentially, beam-splitters and phase-shifters). This

procedure, that is obviously legitimate and will surely be able to generate any pure state, is however not, in general, the most economical one in terms of physical resources. Moreover, this procedure is not particularly insightful because the degrees of bipartite and tripartite entanglement of the resulting output states is not, in general, easily related to the performed operations.

In this section, we want instead to give a precise recipe providing the exact operations to achieve a three-mode pure Gaussian state with any given triplet $\{a_1, a_2, a_3\}$ of local mixedness, and so with any desired ‘physical’ (*i.e.*, constrained by Inequality (5)) asymmetry among the three modes and any needed amount of tripartite entanglement. Clearly, such a recipe is *not* unique. We provide here one possible scheme, which may not be the cheapest one but possesses a straightforward physical interpretation: the distribution, or *allotment* of two-mode entanglement among three modes.

Explicitly, one starts with modes 1 and 2 in a two-mode squeezed state, and mode 3 in the vacuum state, like in Eqs. (55–57). The reason why we choose to have from the beginning a two-mode squeezed state, and not one or more independently squeezed single modes, is that, as already mentioned, two-mode squeezed states can be obtained in the lab [28], either directly in non-degenerate parametric processes or by mixing two squeezed vacua at a beam splitter. The three initial modes are then sent in a sequence of three beam splitters (which we will call “allotment” operator and denote by \hat{A}_{123} , see Fig. 2):

$$\hat{A}_{123} \equiv \hat{B}_{23}(\arccos \sqrt{2/3}) \cdot \hat{B}_{12}(\arccos \sqrt{t}) \cdot \hat{B}_{13}(\arccos \sqrt{s}). \quad (15)$$

It is convenient in this instance to deal with the phase-space representations of the states (*i.e.* their CM) and of the operators (*i.e.* the associated symplectic transformations). The three-mode input state is described by a CM σ_{in}^p of the form Eq. (1) for $n = 3$, with

$$\sigma_1 = \sigma_2 = m \mathbb{1}_2, \quad \sigma_3 = \mathbb{1}_2, \quad (16)$$

$$\varepsilon_{12} = \text{diag} \left\{ \sqrt{m^2 - 1}, -\sqrt{m^2 - 1} \right\}, \quad \varepsilon_{13} = \varepsilon_{23} = \mathbf{0}, \quad (17)$$

and $m \equiv \cosh(2r)$. A beam splitter with transmittivity τ corresponds to a rotation of $\theta = \arccos \sqrt{\tau}$ in phase space, see Eq. (27). In a three-mode system, the symplectic transformation corresponding to $\hat{B}_{ij}(\theta)$ is a direct sum of the matrix $B_{ij}(\tau)$,

$$B_{ij}(\tau) = \begin{pmatrix} \sqrt{\tau} & 0 & \sqrt{1-\tau} & 0 \\ 0 & \sqrt{\tau} & 0 & \sqrt{1-\tau} \\ \sqrt{1-\tau} & 0 & -\sqrt{\tau} & 0 \\ 0 & \sqrt{1-\tau} & 0 & -\sqrt{\tau} \end{pmatrix}, \quad (18)$$

acting on modes i and j , and of the identity $\mathbb{1}_2$ acting on the remaining mode k .

The output state after the allotment will be denoted by a CM σ_{out}^p given by

$$\sigma_{out}^p = A_{123} \sigma_{in}^p A_{123}^\top, \quad (19)$$

where A_{123} is the phase-space representation of the allotment operator Eq. (15), obtained from the matrix product of the three beam-splitter transformations. The output state is clearly pure because the allotment is a unitary operator (symplectic in phase space). The elements of the CM σ_{out}^p , not reported here for brevity, are functions of the three parameters

$$m \in [1, \infty), \quad s \in [0, 1], \quad t \in [0, 1]. \quad (20)$$

In fact, by letting these three parameters vary in their respective domain, the presented procedure allows for the creation of *arbitrary* three-mode pure Gaussian states, with any possible triplet of local mixednesses $\{a_1, a_2, a_3\}$ ranging in the physical region defined by the triangle inequality (5).

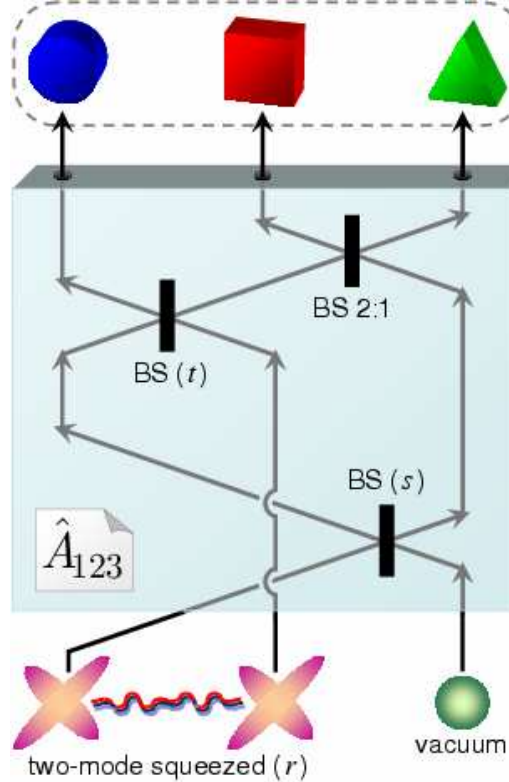


Figure 2. Scheme to produce generic pure three-mode Gaussian states. A two-mode squeezed state and a single-mode vacuum are combined by the “allotment” operator \hat{A}_{123} , which is a sequence of three beam-splitters, Eq. (15). The output yields a generic pure Gaussian state of modes 1 (●), 2 (■), and 3 (▲), whose CM depends on the initial squeezing factor $m = \cosh(2r)$ and on two beam-splitter transmittivities s and t .

This can be shown as follows. Once identified σ_{out}^p with the block form of Eq. (1) (for $n = 3$), one can solve analytically the equation $\text{Det } \sigma_1 = a_1^2$ to find

$$m(a_1, s, t) = \frac{t(t(s-1)^2+s-1)+\sqrt{a_1^2(st+t-1)^2+4s(t-1)t(2t-1)(2st-1)}}{(st+t-1)^2}. \quad (21)$$

Then, substituting Eq. (21) in σ_{out}^p yields a reparametrization of the output state in terms of a_1 (which is given), s and t . Now solve (numerically) the system of nonlinear equations $\{\text{Det } \sigma_2 = a_2^2, \text{Det } \sigma_3 = a_3^2\}$ in the variables s and t . Finally, substitute back the obtained values of the two transmittivities in Eq. (21), to have the desired triplet $\{m, s, t\}$ as functions of the local mixednesses $\{a_1, a_2, a_3\}$ characterizing the target state.

A generic pure three-mode Gaussian state, with a CM locally equivalent to the standard form of Eq. (1) with all diagonal 2×2 subblocks, can thus be produced with the current experimental technology by linear quantum optics, employing the allotment box with exactly tuned amounts of input two-mode squeezing and beam-splitter properties, without any free parameter left. A pictorial test of this procedure is shown in Fig. 3, where at a given local mixedness of mode 1 ($a_1 = 2$), several runs of the allotment operator have been simulated with random beam-splitter of transmittivities s and t . Starting from a two-mode squeezed input with m given by Eq. (21), tensor a vacuum, the resulting output states are plotted in the

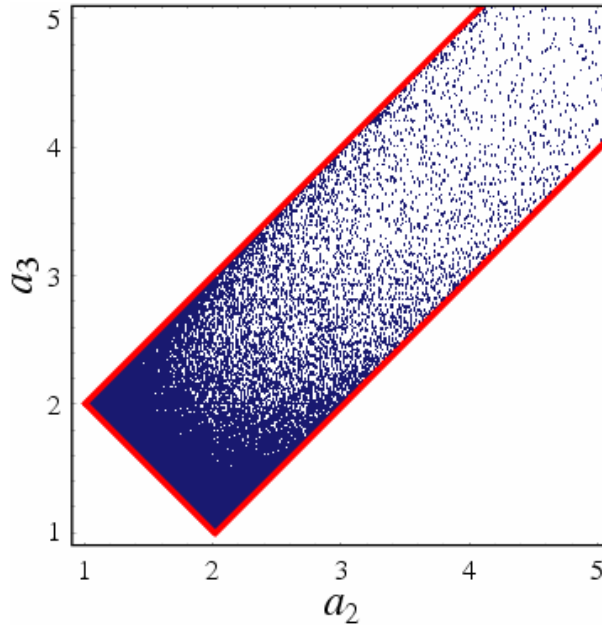


Figure 3. Plot of 100000 randomly generated pure three-mode Gaussian states, described by their single-mode mixednesses a_2 and a_3 , at fixed $a_1 = 2$. The states are produced by simulated applications of the allotment operator with random beam-splitter transmittivities s and t , and span the whole physical range of parameters allowed by Ineq. (5). A comparison of this plot with Fig. 1 of Ref. [2] may be instructive. See text for further details.

space of a_2 and a_3 . By comparing Fig. 3 with Fig. 1 of Ref. [2], one sees clearly that the randomly generated states distribute towards a complete fill of the physical region emerging from the triangle inequality (5), thus confirming the generality of our scheme.

4.2. Continuous-variable GHZ/W states

Some of us have previously shown [15] a quite surprising feature associated with the structure of entanglement sharing in CV systems. Namely, when trying to define, within the class of fully symmetric Gaussian states – with CM Eq. (7) –, the CV counterparts of the inequivalent states $|\psi_{\text{GHZ}}\rangle$ and $|\psi_W\rangle$ of three qubits, if one aims at maximizing (at given single-mode mixedness $a = \sqrt{\text{Det } \alpha}$) either the two-mode entanglement $G_{\tau}^{i|j}$ in any reduced state (*i.e.* aiming at the CV ‘W-like’ state), or the genuine tripartite entanglement G_{τ}^{res} (*i.e.* aiming at the CV ‘GHZ-like’ state), one finds the same, unique family of states. These pure fully symmetric three-mode Gaussian states, previously known as CV ‘GHZ-type’ states [29, 30, 12], have been thus renamed ‘CV GHZ/W states’ [15, 2, 31]. They are described by a CM σ_s^p of the form Eq. (7), with $\alpha = a \mathbb{1}_2$, $\varepsilon = \text{diag}\{e^+, e^-\}$ and [16]

$$e^{\pm} = \frac{a^2 - 1 \pm \sqrt{(a^2 - 1)(9a^2 - 1)}}{4a}, \quad (22)$$

ensuring the global purity of the state. In the limit of infinite squeezing ($a \rightarrow \infty$), CV GHZ/W states approach the proper (unnormalizable) continuous-variable GHZ state $\int dx|x, x, \dots, x\rangle$, a simultaneous eigenstate of total momentum $\hat{p}_1 + \hat{p}_2 + \hat{p}_3$ and all relative positions $\hat{x}_i - \hat{x}_j$ ($i, j = 1, 2, 3$), with zero eigenvalues [32].

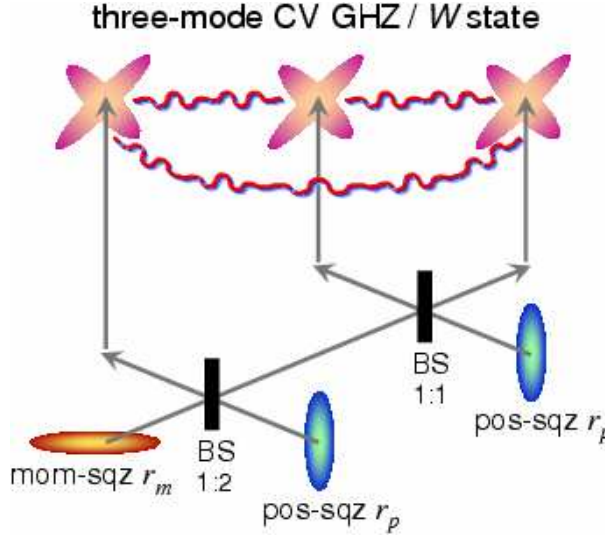


Figure 4. Scheme to produce CV GHZ/W states, as proposed in Ref. [29] and implemented in Ref. [18]. Three independently squeezed beams, one in position and two in momentum, are combined through a double beam splitter (tritter). The output yields a pure, symmetric, fully inseparable three-mode Gaussian state, also known as CV GHZ/W state.

Arravagliament. The tripartite entanglement of finite-squeezing GHZ/W states, as measured by the residual Gaussian contangle Eq. (13), simply reads [15]

$$G_{\tau}^{res}(\sigma_s^p) = \text{arcsinh}^2 \left[\sqrt{a^2 - 1} \right] - \frac{1}{2} \log_2 \left[\frac{3a^2 - 1 - \sqrt{9a^4 - 10a^2 + 1}}{2} \right], \quad (23)$$

and it is greater than zero as soon as $a > 1$, for which these states are fully inseparable [1, 16, 29, 33, 12]. For GHZ/W states the residual Gaussian contangle G_{τ}^{res} Eq. (13) coincides with the true residual contangle E_{τ}^{res} Eq. (12), as the Gaussian pure-state decomposition is the optimal one in every bipartition (due to the global purity of the state and to the symmetry of the two-mode reductions).

State engineering. Several schemes have been proposed [34] to produce what we call GHZ/W states of continuous variables. In particular, as discussed by Van Loock and Braunstein [29], these states can be produced by mixing three squeezed beam in a double beam splitter, or *tritter* [35]. One starts with mode 1 squeezed in momentum, and modes 2 and 3 squeezed in position. In Heisenberg picture:

$$\hat{x}_1 = e^{r_m} \hat{x}_1^0, \quad \hat{p}_1 = e^{-r_m} \hat{p}_1^0, \quad (24)$$

$$\hat{x}_{2,3} = e^{-r_p} \hat{x}_{2,3}^0, \quad \hat{p}_{2,3} = e^{r_p} \hat{p}_{2,3}^0, \quad (25)$$

where the suffix “0” refers to the vacuum. Then one combines the three modes in a tritter

$$\hat{B}_{123} \equiv \hat{B}_{23}(\pi/4) \cdot \hat{B}_{12}(\arccos \sqrt{1/3}), \quad (26)$$

where the action of an ideal (phase-free) beam splitter operation \hat{B}_{ij} on a pair of modes i and j is defined as

$$\hat{B}_{ij}(\theta) : \begin{cases} \hat{a}_i \rightarrow \hat{a}_i \cos \theta + \hat{a}_j \sin \theta \\ \hat{a}_j \rightarrow \hat{a}_i \sin \theta - \hat{a}_j \cos \theta \end{cases}, \quad (27)$$

with $\hat{a}_l = (\hat{x}_l + i\hat{p}_l)/2$ being the annihilation operator of mode k , and θ the angle in phase space ($\theta = \pi/4$ corresponds to a 50:50 beam splitter).

The output of the tritter yields a CM of the form Eq. (7) with

$$\boldsymbol{\alpha} = \text{diag} \left\{ \frac{1}{3} (e^{2r_m} + 2e^{-2r_p}), \quad \frac{1}{3} (e^{-2r_m} + 2e^{2r_p}) \right\}, \quad (28)$$

$$\boldsymbol{\varepsilon} = \text{diag} \left\{ \frac{1}{3} (e^{2r_m} - e^{-2r_p}), \quad \frac{1}{3} (e^{-2r_m} - e^{2r_p}) \right\}. \quad (29)$$

This resulting pure and fully symmetric three-mode Gaussian state, obtained in general with differently squeezed inputs $r_m \neq r_p$, is locally equivalent to the state prepared with all initial squeezings equal to the average $\bar{r} = (r_m + r_p)/2$ [36].

The CM described by Eqs. (28,29) represents a CV GHZ/W state. It can be in fact transformed, by local symplectic operations, into the standard form CM Eq. (22) with

$$a = \frac{1}{3} \sqrt{4 \cosh [2(r_m + r_p)] + 5}. \quad (30)$$

The preparation scheme of CV GHZ/W states is depicted in Fig. 4. It has been experimentally implemented [18], and the fully inseparability of the produced states has been verified through the violation of Ineq. (4) [12]. Very recently, the production of strongly entangled GHZ/W states has also been demonstrated by using a novel optical parametric oscillator (OPO), based on concurrent $\chi^{(2)}$ nonlinearities [19].

4.3. *T* states with zero reduced bipartite entanglement

Further insight into this peculiar entanglement sharing structure is obtained from the maximization of the 1×2 bipartite Gaussian contangle $G_{\tau}^{i|(jk)}$ under the constraint of separability of all two-mode reductions. The resulting family of Gaussian states fulfilling this request is constituted by symmetric mixed states which have been named *T states* [*T* standing for *tripartite* (entanglement only)] in Ref. [2], described by a CM $\boldsymbol{\sigma}_s^T$ of the form Eq. (7), with $\boldsymbol{\alpha} = a\mathbb{1}_2$, $\boldsymbol{\varepsilon} = \text{diag}\{e^+, e^-\}$ and

$$e^+ = \frac{a^2 - 5 + \sqrt{9a^2(a^2 - 2) + 25}}{4a}, \quad e^- = \frac{5 - 9a^2 + \sqrt{9a^2(a^2 - 2) + 25}}{12a}. \quad (31)$$

Arravagliament. The *T* states, like the GHZ/W states, are determined only by the local mixedness a , and are fully separable for $a = 1$ and fully inseparable for all $a > 1$. The residual Gaussian contangle Eq. (13), as a function of a , can be analytically computed for these states exploiting the unitary localization procedure (see Fig. 1) for the evaluation of the 1×2 entanglement. As shown in Ref. [2], the tripartite entanglement G_{τ}^{res} for *T* states is

$$\begin{aligned} G_{\tau}^{res}(\boldsymbol{\sigma}_s^T) = & \text{arcsinh}^2 \left\{ \left[-9a^4 + 3Ra^2 + 6a^2 + 25R - 109 \right. \right. \\ & - \sqrt{2} \left(81a^8 - 432a^6 + 954a^4 - 1704a^2 + 2125 \right. \\ & \left. \left. - (3a^2 - 11)(3a^2 - 7)(3a^2 + 5)R \right)^{\frac{1}{2}} \right]^{\frac{1}{2}} \\ & \times \left[18(3a^2 - R + 3) \right]^{-\frac{1}{2}} \left. \right\}, \end{aligned} \quad (32)$$

with $R \equiv \sqrt{9a^2(a^2 - 2) + 25}$.

Comparing Eq. (32) with Eq. (23) (see also Ref. [2]) one finds that the arravagliamento of T states is strictly smaller than the one of GHZ/W states, at a given degree of local mixedness a . This confirmatory evidence of what is known as the *promiscuity* of entanglement sharing in symmetric Gaussian states [15], entails remarkable consequences both on a basic and on an applicative point of view, which will be investigated in the following.

State engineering. It may be useful to know how to produce this novel class of mixed Gaussian states in the lab. The simplest way to engineer T states is to reutilize the scheme of Fig. 4, *i.e.* basically the tritter, but with different inputs. Namely, one has mode 1 squeezed again in momentum (with squeezing parameter r), but this time modes 2 and 3 are in a thermal state (with average photon number $\bar{n} = [n(r) - 1]/2$, depending on r). In Heisenberg picture:

$$\hat{x}_1 = e^r \hat{x}_1^0, \quad \hat{p}_1 = e^{-r} \hat{p}_1^0, \quad (33)$$

$$\hat{x}_{2,3} = \sqrt{n(r)} \hat{x}_{2,3}^0, \quad \hat{p}_{2,3} = \sqrt{n(r)} \hat{p}_{2,3}^0, \quad (34)$$

$$\text{with } n(r) = \sqrt{3 + e^{-4r}} - e^{-2r}.$$

Sending these three modes in a tritter Eq. (26) one recovers, at the output, a T state whose CM is locally equivalent to the standard form of Eq. (31), with

$$a = \frac{1}{3} \sqrt{2e^{-2r} \sqrt{3 + e^{-4r}} (-3 + e^{4r}) + 6e^{-4r} + 11}. \quad (35)$$

4.4. Promiscuous entanglement sharing: The power of symmetric resources

Our inspection shows that, in symmetric three-mode Gaussian states, when there is no two-mode entanglement (like in T states), the genuine tripartite one is not enhanced, but frustrated. Instead, if a mode is “maximally entangled” with another, it can also achieve maximal quantum correlations in a three-party relation (like in GHZ/W states). Such an unparalleled feature (at striking variance with the behaviour of quantum correlations distributed among qubits) hints at the “*promiscuous*” nature of CV entanglement sharing in symmetric Gaussian states [15, 26, 31, 2].

This theoretical evidence strongly promotes GHZ/W states, experimentally realizable with the current technology [18, 19], as paradigmatic candidates for reliable CV quantum communication [31]. Exploiting a strongly entangled three-mode CV GHZ/W state as a quantum channel affords one with a number of simultaneous advantages:

- (i) the “guaranteed success” (*i.e.* with better-than-classical figures of merit) of any tripartite quantum information protocol like teleportation network [29, 37, 36], secret sharing [38], controlled dense coding [39] or Byzantine agreement [40];
- (ii) the “guaranteed success” of any standard two-user CV protocol, because a highly entangled two-mode channel is readily available after a unitary (reversible) localization [10] has been performed through a single beam splitter (see Fig. 1);
- (iii) the “guaranteed success” (though with nonmaximal efficiency) of any two-party quantum protocol through each two-mode channel obtained discarding one of the three modes.

An explicit implementation of this checklist will be provided in Section 6.2, where it will be also shown that the arravagliamento in the class of GHZ/W states acquires a clear operative interpretation in terms of the optimal fidelity of three-party CV teleportation networks [36].

Point (iii) is realized with nonmaximal efficiency because, while the genuine tripartite contangle Eq. (23) of GHZ/W states diverges in the limit of infinite squeezing ($a \rightarrow \infty$), the reduced entanglement in any two-mode partition remains finite, and saturates to the value

$$G_{\tau}^{i|j}(\sigma_s^p, a \rightarrow \infty) = \frac{\log_2 3}{4} \approx 0.3. \quad (36)$$

This intrinsic limitation *per sé* establishes Inequality (8) for GHZ/W states in the asymptotic regime, preventing a *polygamous* CV entanglement which, though appealing as a concept, is forbidden by Quantum Mechanics [26].

A natural question arises in this context, namely whether *all* three-mode Gaussian states host a promiscuous distribution of entanglement. We will now show with specific examples that this is not the case, in that a traditional entanglement sharing is restored as soon as the full symmetry of the states is dropped; in the symmetric instance, though, we will show that even a strong amount of global mixedness and/or noise is typically unable to destroy the promiscuous entanglement sharing. This observation, together with the finding that fully symmetric states (CV GHZ/W states) are the most robust three-mode Gaussian states against decoherence effects (see Ref. [2] and Sec. 6.3), concretely supports the opportunity of employing these states as channels for current and maybe novel quantum information protocols with continuous variables.

4.5. Noisy GHZ/W states: The effect of mixedness

In the experimental practice, no perfectly pure state can be generated, because of the action of environmental noise during the state's creation process. In the Gaussian setting, such an action can be simply modeled by assuming that an initial thermal state (instead of a pure vacuum) undergoes the same Gaussian operations needed to create its pure counterpart. We consider here the noisy version of the GHZ/W states previously introduced (Sec. 4.2), which are a family of mixed Gaussian fully symmetric states, also called three-mode squeezed thermal states [41]. Let us mention that various properties of noisy three-mode Gaussian states have already been addressed, mainly regarding their effectiveness in the implementation of CV protocols [42, 43]. Here, we focus on the multipartite entanglement properties of noisy states. This analysis will allow us to go beyond the set of pure states, thus gaining deeper insight into the role played by realistic quantum noise in the sharing and characterization of tripartite entanglement.

Noisy GHZ/W states are described by a CM σ_s^{th} of the form Eq. (7), with $\alpha = a\mathbb{1}_2$, $\varepsilon = \text{diag}\{e^+, e^-\}$ and

$$e^\pm = \frac{a^2 - n^2 \pm \sqrt{(a^2 - n^2)(9a^2 - n^2)}}{4a}. \quad (37)$$

Noisy GHZ/W states have a completely degenerate symplectic spectrum (their symplectic eigenvalues being all equal to n) and represent thus, somehow, the three-mode generalization of two-mode squeezed thermal states (also known as symmetric GMEMS, states of maximal negativity at fixed purities [44, 45, 46]). The state σ_s^{th} is completely determined by the local purity $\mu_l = a^{-1}$ and by the global purity $\mu = n^{-3}$. Noisy GHZ/W states reduce to pure GHZ/W states (*i.e.* squeezed *vacuum* states) for $n = 1$.

State engineering. As already remarked, noisy GHZ/W states can be obtained as GHZ/W states generated from (Gaussian) thermal states: one starts with three single-mode squeezed thermal states (with average photon number $\bar{n} = [n - 1]/2$) and combine them through a tritter Eq. (26), with the same procedure described in Fig. 4 for $n = 1$. The initial single, separable, modes are thus described by the following operators:

$$\hat{x}_1 = \sqrt{n}e^r \hat{x}_1^0, \quad \hat{p}_1 = \sqrt{n}e^{-r} \hat{p}_1^0, \quad (38)$$

$$\hat{x}_{2,3} = \sqrt{n}e^{-r} \hat{x}_{2,3}^0, \quad \hat{p}_{2,3} = \sqrt{n}e^r \hat{p}_{2,3}^0. \quad (39)$$

Defining $s \equiv e^{2r}$, at the output of the tritter one obtains a CM of the form Eq. (7), with

$$\alpha = \text{diag} \left\{ \frac{n(s^2 + 2)}{3s}, \quad \frac{n(2s^2 + 1)}{3s} \right\}, \quad (40)$$

$$\boldsymbol{\varepsilon} = \text{diag} \left\{ \frac{n(s^2 - 1)}{3s}, -\frac{n(s^2 - 1)}{3s} \right\}. \quad (41)$$

This resulting CM is locally equivalent to the standard form of Eq. (37), with

$$a = \frac{n\sqrt{2s^4 + 5s^2 + 2}}{3s}. \quad (42)$$

Let us also mention that noisy GHZ/W states would also result from the dissipative evolution of pure GHZ/W states in proper Gaussian noisy channels [2].

Entanglement properties. Depending on the parameters s and n , noisy GHZ/W states can belong to three different separability classes [1] (and not to only two classes like the previously considered examples). Namely, as explicitly computed in Ref. [41], we have in our notation

$$s > \frac{\sqrt{9n^4 - 2n^2 + 9 + 3(n^2 - 1)\sqrt{9n^4 + 14n^2 + 9}}}{4n} \Rightarrow \text{class 1}; \quad (43)$$

$$n < s \leq \frac{\sqrt{9n^4 - 2n^2 + 9 + 3(n^2 - 1)\sqrt{9n^4 + 14n^2 + 9}}}{4n} \Rightarrow \text{class 4}; \quad (44)$$

$$s \leq n \Rightarrow \text{class 5}. \quad (45)$$

States which fulfill Ineq. (43) are fully inseparable (*i.e.* with genuine tripartite entanglement), while states that violate it are PPT. However, as already mentioned, PPTness does not imply separability [1]. In fact, in the range defined by Ineq. (44), noisy GHZ/W states are three-mode biseparable, that is they exhibit tripartite *bound entanglement*. This can be verified by showing, using the methods of Ref. [1], that such states cannot be written as a convex combination of separable states. Finally, noisy GHZ/W states that fulfill Ineq. (45) are fully separable, containing no entanglement at all.

The tripartite residual Gaussian contangle Eq. (13), which is nonzero only in the fully inseparable region, can be explicitly computed. In particular, the 1×2 Gaussian contangle $G_{\tau}^{i|(jk)}$ is obtained following a similar strategy to that employed for T states (see Sec. 4.3). Namely, if one performs a unitary localization on modes 2 and 3 that decouples the transformed mode 3', one finds that the resulting equivalent two-mode state of modes 1 and 2' is symmetric. The bipartite Gaussian contangle of the three-mode state follows then from Eq. (11). As for the two-mode Gaussian contangles $G_{\tau}^{1|2} = G_{\tau}^{1|3}$, the same formula can be used, as the reduced states are symmetric. Finally one gets, in the range defined by Ineq. (43), an arravagliament given by

$$G_{\tau}^{\text{res}}(\boldsymbol{\sigma}_s^{\text{th}}) = \frac{1}{4} \log_2 \left\{ \frac{n^2 [4s^4 + s^2 + 4 - 2(s^2 - 1)\sqrt{4s^4 + 10s^2 + 4}]}{9s^2} \right\} - 2 \left[\max \left\{ 0, -\log_2 \left(\frac{n\sqrt{s^2 + 2}}{\sqrt{3s}} \right) \right\} \right]^2, \quad (46)$$

and $G_{\tau}^{\text{res}}(\boldsymbol{\sigma}_s^{\text{th}}) = 0$ when Ineq. (43) is violated. For noisy GHZ/W states, the residual Gaussian contangle Eq. (46) is still equal to the true one (like in the special instance of GHZ/W states), thanks to the symmetry of the two-mode reductions, and of the unitarily transformed state of modes 1 and 2'.

Sharing structure. The second term in Eq. (46) embodies the sum of the couplewise entanglement in the $1|2$ and $1|3$ reduced bipartitions. Therefore, if its presence enhances the value of the tripartite residual contangle (as compared to what happens if it vanishes), then

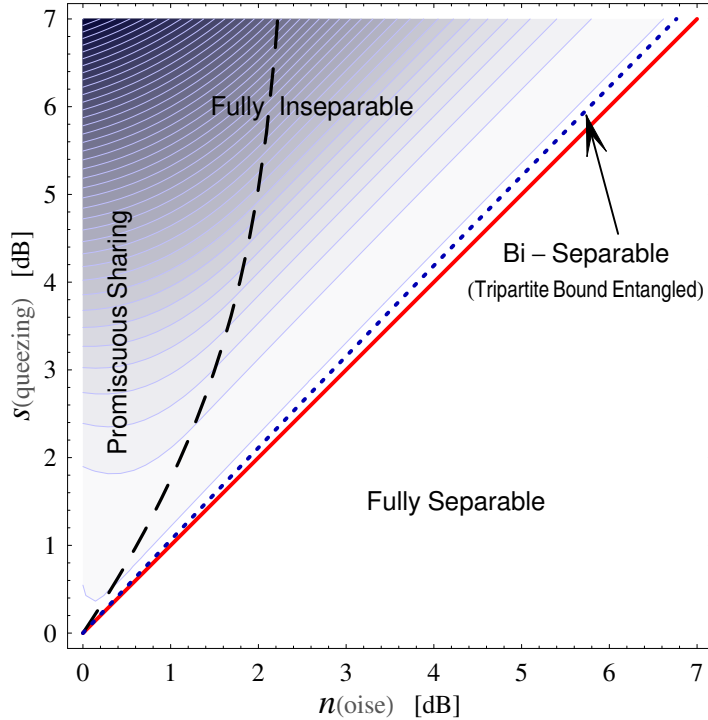


Figure 5. Summary of separability and entanglement properties of three-mode squeezed thermal states, or noisy GHZ/W states, in the space of the two parameters n and s [see Eqs. (38–41)]. The separability is classified according to the scheme of Ref. [1]. Above the dotted line the states are fully inseparable (class 1); below the solid line they are fully separable (class 5). In the narrow intermediate region, noisy GHZ/W states are three-mode biseparable (class 4), *i.e.* they exhibit tripartite bound entanglement. The relations defining the boundaries for the different regions are given in Eqs. (43–45). In the fully inseparable region, the residual (Gaussian) contangle Eq. (46) is depicted as a contour plot, growing with increasing darkness from $G_\tau^{res} = 0$ (along the dotted line) to $G_\tau^{res} \approx 1.9$ (at $n = 0$ dB, $s = 7$ dB [47]). On the left side of the dashed line, whose expression is given by Eq. (48), not only genuine tripartite entanglement is present, but also each reduced two-mode bipartition is entangled. In this region, G_τ^{res} is strictly larger than in the region where the two-mode reductions are separable. This evidences the *promiscuous* sharing structure of multipartite CV entanglement in symmetric, even mixed, three-mode Gaussian states.

one can infer that entanglement sharing is ‘promiscuous’ in the (mixed) three-mode squeezed thermal Gaussian states as well (‘noisy GHZ/W’ states). And this is exactly the case, as shown in the contour plot of Fig. 5, where the separability and entanglement properties of noisy GHZ/W states are summarized. Explicitly, one finds that for

$$n \geq \sqrt{3}, \quad (47)$$

the entanglement sharing can never be promiscuous, as the reduced two-mode entanglement is zero for any (even arbitrarily large) squeezing s . Otherwise, applying PPT criterion to any two-mode reduction one finds that for sufficiently high squeezing bipartite entanglement is also present in any two-mode reduction, namely

$$n < \sqrt{3}, \quad s > \frac{\sqrt{2}n}{\sqrt{3-n^2}} \quad \Rightarrow \quad \text{promiscuous sharing.} \quad (48)$$

Evaluation of Eq. (46), as shown in Fig. 5, clearly demonstrates that the genuine tripartite entanglement increases with increasing bipartite entanglement in any two-mode reduction, unambiguously confirming that CV quantum correlations distribute in a promiscuous way not only in pure [15], but also in *mixed* symmetric three-mode Gaussian states. However, the global mixedness is prone to affect this sharing structure, which is completely destroyed if, as can be seen from Eq. (47), the global purity μ falls below $1/(3\sqrt{3}) \approx 0.19245$. This purity threshold is remarkably low: a really strong amount of global noise is necessary to destroy the promiscuity of entanglement distribution.

4.6. Basset-hound states: A ‘traditional’ sharing of entanglement

Let us finally consider an instance of tripartite entangled states which are not fully symmetric, but merely bisymmetric pure Gaussian states. Following the arguments summarized in Fig. 1, they will be named *basset-hound* states. Such states are denoted by a CM σ_B^p of the form Eq. (1) for $n = 3$, with

$$\sigma_1 = a \mathbb{1}_2, \quad \sigma_2 = \sigma_3 = \left(\frac{a+1}{2} \right) \mathbb{1}_2, \quad (49)$$

$$\varepsilon_{23} = \left(\frac{a-1}{2} \right) \mathbb{1}_2, \quad \varepsilon_{12} = \varepsilon_{13} = \text{diag} \left\{ \frac{\sqrt{a^2-1}}{\sqrt{2}}, -\frac{\sqrt{a^2-1}}{\sqrt{2}} \right\}. \quad (50)$$

They belong to a family of states introduced in Ref. [48] as resources for optimal CV telecloning (*i.e.* cloning at distance, or equivalently teleportation to more than one receiver) of single-mode coherent states. A more detailed discussion of this protocol will be given in Sec. 7.

Arravagliament. From a qualitative point of view, basset-hound states are fully inseparable for $a > 1$ and fully separable for $a = 1$, as already remarked in Ref. [48]; moreover, the PPT criterion entails that the two-mode reduced state of modes 2 and 3 is always separable. Following the guidelines of Sec. 3.2, the residual Gaussian contangle G_τ^{res} is easily computable. From Eq. (14), it follows that the minimum in Eq. (13) is attained if one sets either mode 2 or mode 3 (indifferently, due to the bisymmetry) to be the reference mode. Let us choose mode 3; then we have

$$G_\tau^{res}(\sigma_B^p) = G_\tau^{3|(12)}(\sigma_B^p) - G_\tau^{3|1}(\sigma_B^p), \quad (51)$$

with

$$G_\tau^{3|(12)}(\sigma_B^p) = \text{arcsinh}^2 \left[\frac{1}{2} \sqrt{(a-1)(a+3)} \right], \quad (52)$$

$$G_\tau^{3|1}(\sigma_B^p) = \text{arcsinh}^2 \left[\sqrt{\frac{(3a+1)^2}{(a+3)^2} - 1} \right]. \quad (53)$$

The tripartite entanglement Eq. (51) is strictly smaller than that of both GHZ/W states and T states, but it can still diverge in the limit of infinite squeezing ($a \rightarrow \infty$) due to the global purity of basset-hound states. Instead, the bipartite entanglement $G_\tau^{1|2} = G_\tau^{1|3}$ between mode 1 and each of the modes 2 and 3 in the corresponding two-mode reductions, given by Eq. (53), is strictly *larger* than the bipartite entanglement in any two-mode reduction of GHZ/W states. This does not contradict the previously given characterization of GHZ/W states as maximally three-way and two-way entangled (maximally promiscuous). In fact, GHZ/W states have maximal couplewise entanglement between *any* two-mode reduction, while in basset-hound states only two (out of three) two-mode reductions are entangled, allowing this entanglement

to be larger. This is the reason why these states are well-suited for telecloning, as we will detail in Sec. 7.1. Nevertheless, this reduced bipartite entanglement cannot increase arbitrarily in the limit of infinite squeezing, because of the monogamy inequality (8); in fact it saturates to

$$G_{\tau}^{1|l}(\sigma_B^p, a \rightarrow \infty) = \log_2^2 [3 + 2\sqrt{2}] \approx 3.1, \quad (54)$$

which is about ten times the asymptotic value of the reduced bipartite two-mode entanglement for GHZ/W states, Eq. (36).

Sharing structure. It is interesting to notice that entanglement sharing in basset-hound states is *not* promiscuous. Tripartite and bipartite entanglement coexist (the latter only in two of the three possible two-mode reductions), but the presence of a strong bipartite entanglement does not help the tripartite one to be stronger (at fixed local mixedness a) than in other states, like GHZ/W states or even T states (which are globally mixed and moreover contain no reduced bipartite entanglement at all).

This is a clear hint that, in the Gaussian setting, ‘*promiscuity*’ is a peculiar consequence not of the global purity (noisy GHZ/W states remain promiscuous for quite strong mixedness), but of the complete *symmetry* under modes-exchange. Beside frustrating the maximal entanglement between pairs of modes [49], symmetry also constrains the multipartite sharing of quantum correlations. In basset-hound states, the separability of the reduced state of modes 2 and 3 prevents the three modes from having a strong arravagliament among them all, despite the heavy quantum correlations shared by the two couples of modes 1|2 and 1|3.

State engineering. A scheme for producing basset-hound states, and in general the whole family of states useful for telecloning (known as “multiuser quantum channels”), is provided in Ref. [48]. In the case of basset-hound states of the form given by Eqs. (49,50), one starts with a two-mode squeezed state (with squeezing parameter r) and a single-mode vacuum. Let us recall, again, that the two-mode squeezed state can be obtained as usual by superimposing two independently squeezed single modes (one in momentum and the other in position) at a 50:50 beam splitter, or can be produced directly as a twin beam using *e.g.* a type-II OPO [28]. In Heisenberg picture:

$$\hat{x}_1 = \frac{1}{\sqrt{2}} (e^r \hat{x}_1^0 + e^{-r} \hat{x}_2^0), \quad \hat{p}_1 = \frac{1}{\sqrt{2}} (e^{-r} \hat{p}_1^0 + e^r \hat{p}_2^0), \quad (55)$$

$$\hat{x}_2 = \frac{1}{\sqrt{2}} (e^r \hat{x}_1^0 - e^{-r} \hat{x}_2^0), \quad \hat{p}_2 = \frac{1}{\sqrt{2}} (e^{-r} \hat{p}_1^0 - e^r \hat{p}_2^0), \quad (56)$$

$$\hat{x}_3 = \hat{x}_3^0, \quad \hat{p}_3 = \hat{p}_3^0. \quad (57)$$

Then, one combines one half of the two-mode squeezed state with the vacuum mode via a 50:50 beam splitter. The resulting three-mode state is exactly a basset-hound state described by Eqs. (49,50), once one identifies $a = \cosh(2r)$. In a realistic setting, dealing with noisy input modes, mixed basset-hound states can be obtained as well by the same procedure.

5. Application: Multiparty quantum teleportation with continuous variables

We now discuss more closely the usefulness of three-mode Gaussian states for the efficient implementation of quantum information and communication protocols. Let us mention that tripartite entangled Gaussian states have been successfully exploited to demonstrate quantum secret sharing [38] and controlled dense coding [39] for continuous variables. Recently, a theoretical solution for CV Byzantine agreement has been reported [40], based on the use of sufficiently entangled states from the family of CV GHZ/W states. Here, we intend to

epitomize the capability of Gaussian states for quantum communication and to provide their theoretical entanglement characterization with a significant operative background. To this aim we shall focus on the transmission of quantum states by classical communication, within a network of three parties which share entangled Gaussian resources.

For two parties, the process of *quantum teleportation* using entanglement and with the aid of classical communication was originally proposed for qubit systems [50], and experimentally implemented with polarization-entangled photons [51, 52]. The CV counterpart of discrete-variable teleportation, using quadrature entanglement, is in principle imperfect due to the impossibility of achieving infinite squeezing. Nevertheless, by considering the finite EPR correlations between the quadratures of a two-mode squeezed Gaussian state, a realistic scheme for CV teleportation (see Ref. [53] for a recent review) was proposed [54, 55] and experimentally implemented [56] to teleport coherent states with a measured fidelity $\mathcal{F} = 0.70 \pm 0.02$ [57]. Without using entanglement, by purely classical communication, an average fidelity of

$$\mathcal{F}_{cl} = \frac{1}{2} \quad (58)$$

is the best that can be achieved with a coherent alphabet of input states [58, 59]. Let us recall that the fidelity \mathcal{F} , which is the figure of merit quantifying the success of a teleportation experiment, is defined with respect to a pure state $|\psi^{in}\rangle$ as

$$\mathcal{F} \equiv \langle \psi^{in} | \rho^{out} | \psi^{in} \rangle. \quad (59)$$

Here “in” and “out” denote the input and the output states (the latter being generally mixed) of a teleportation process, respectively. \mathcal{F} reaches unity only for a perfect state transfer, $\rho^{out} = |\psi^{in}\rangle\langle\psi^{in}|$. To accomplish teleportation with high fidelity, the sender (Alice) and the receiver (Bob) must share an entangled state (resource). The *sufficient* fidelity criterion [58] states that, if teleportation is performed with $\mathcal{F} > \mathcal{F}_{cl}$, then the two parties exploited an entangled state. The converse is generally false, that is, quite surprisingly, some entangled resources may yield lower-than-classical fidelities [36, 29]. This point will be discussed thoroughly in the following.

To generalize the process of CV teleportation from two to three (and more) users, one can consider two basic possible scenarios. On the one hand, a network can be created where each user is able to teleport states with better-than-classical efficiency (being the same for all sender/receiver pairs) to any chosen receiver *with the assistance of the other parties*. On the other hand, one of the parties acts as the fixed sender, and distributes many approximate copies (with in principle different cloning fidelities) to all the others acting as remote receivers. These two protocols, respectively referred to as “teleportation network” [29] and “telecloning” [48], will be described in the two following sections, and the connections between their successful implementation with three-mode Gaussian resources and the amounts of shared bipartite and tripartite entanglement will be elucidated. We just mention that several interesting variants to these basic schemes do exist, (see, *e.g.* the ‘cooperative telecloning’ of Ref. [60], where two receivers – instead of two senders – are cooperating).

6. Teleportation networks with fully symmetric resources

The original CV teleportation protocol [55] has been generalized to a multi-user teleportation network requiring multiparty entangled Gaussian states in Ref. [29]. This network has been recently experimentally demonstrated by exploiting three-mode squeezed states (namely, noisy CV GHZ/W states, extensively addressed in section 4.5, were employed), yielding a maximal fidelity $\mathcal{F} = 0.64 \pm 0.02$ [37].

6.1. Equivalence between multipartite entanglement and optimal fidelity

Let us consider the instance of a N -mode teleportation-network protocol, involving N users who share a genuine N -partite entangled Gaussian resource, completely symmetric under permutations of the modes [29]. Two parties are randomly chosen as sender (Alice) and receiver (Bob), but, in order to accomplish teleportation of an unknown coherent state, Bob needs the results of $N - 2$ momentum detections performed locally by each of the other cooperating parties on their own subsystems. Under the assumption of perfect symmetry under mode permutation, a nonclassical teleportation fidelity (i.e. $\mathcal{F} > \mathcal{F}^{cl}$) between *any* pair of parties is sufficient for the presence of genuine N -partite entanglement in the shared resource, while in general the converse is false (see, *e.g.*, Fig. 1 of Ref. [29]).

In Ref. [36] the problem was raised of determining the *optimal* multi-user teleportation fidelity, and to extract from it a quantitative information on the multipartite entanglement in the shared resource. The optimization consists in a maximization of the fidelity over all local single-mode operations ('pre-processing' the initial resource), at fixed amounts of noise and entanglement in the shared resource. Let us consider realistically mixed N -mode Gaussian resources, obtained by combining a mixed momentum-squeezed state (with squeezing parameter r_m) and $N - 1$ mixed position-squeezed states (with squeezing parameter r_p and in principle a different noise factor) into an N -splitter [29], which is a sequence of $N - 1$ suitably tuned beam splitters:

$$\begin{aligned} \hat{B}_{1\dots N} \equiv & \hat{B}_{N-1,N}(\pi/4) \cdot \hat{B}_{N-2,N-1} \left(\arccos \sqrt{1/3} \right) \cdot \dots \\ & \cdot \hat{B}_{2,3} \left(\arccos \sqrt{1/(N-1)} \right) \cdot \hat{B}_{1,2} \left(\arccos \sqrt{1/N} \right). \end{aligned} \quad (60)$$

In Heisenberg picture, the input modes are

$$\hat{x}_1 = \sqrt{n_m} e^{r_m} \hat{x}_1^0, \quad \hat{p}_1 = \sqrt{n_m} e^{-r_m} \hat{p}_1^0, \quad (61)$$

$$\hat{x}_{2,3,\dots,N} = \sqrt{n_p} e^{-r_p} \hat{x}_{2,3,\dots,N}^0, \quad \hat{p}_{2,3,\dots,N} = \sqrt{n_p} e^{r_p} \hat{p}_{2,3,\dots,N}^0. \quad (62)$$

The resulting state after the N -splitter is a completely symmetric mixed Gaussian state of a N -mode CV system, reducing to a three-mode squeezed thermal state (noisy GHZ/W state, see Sec. 4.5) for $N = 3$.

For a given thermal noise in the individual modes, all the states with equal average squeezing

$$\bar{r} \equiv \frac{r_m + r_p}{2} \quad (63)$$

are equivalent up to local single-mode unitary operations and possess, by definition, the same amount of bipartite and multipartite entanglement with respect to any partition. The teleportation efficiency, instead, depends separately on the different single-mode squeezings. This is crucial: in all the subsections dedicated to state engineering in Sec. 4, we provided schemes for the generation of states with CMs *locally equivalent* to the corresponding standard forms. While all the states belonging to the same local-equivalence class are undistinguishable from the point of view of their entanglement properties, *they generally behave differently when employed in quantum information and communication processes*, for which the optical phase reference gets relevant. However, as first shown in Ref. [36], the optimal fidelity achievable with a symmetric multimode Gaussian resource by local pre-processing is *equivalent* to the degree of multipartite entanglement contained in the resource. We will now briefly recall this finding, and discuss it with an especial care towards the experimental implications for three-mode states, also in the light of the results on tripartite CV entanglement reported in the previous sections and in Ref. [2].

Because the entanglement in the multimode resources shared for a teleportation network only depends on \bar{r} Eq. (63), we have the freedom of unbalancing the local squeezings r_m and r_p , *i.e.* to tune their semidifference

$$d \equiv \frac{r_m - r_p}{2} \quad (64)$$

from the beginning, at fixed \bar{r} . Without affecting the entanglement, we want then to single out the optimal form of the resource state, which enables a teleportation network with maximal fidelity. This analysis is straightforward (see Ref. [36] for details), and yields an optimal difference $d = d_N^{opt}$ between the single-mode squeezings of

$$d_N^{opt} = \bar{r} + \frac{1}{4} \log_2 \left[\frac{N}{(N-2) + 2 \frac{n_p}{n_m} e^{4\bar{r}}} \right]. \quad (65)$$

The corresponding optimal teleportation-network fidelity reads [36]

$$\mathcal{F}_N^{opt} = \frac{1}{1 + \tilde{\nu}_-^{(N)}}, \quad \tilde{\nu}_-^{(N)} \equiv \sqrt{\frac{N n_m n_p}{2 e^{4\bar{r}} + (N-2) n_m / n_p}}. \quad (66)$$

Before commenting on the significance of the quantity $\tilde{\nu}_-^{(N)}$, let us briefly discuss the form of the resource states which enable teleportation networks with maximal fidelity. The optimal form of the shared N -mode symmetric Gaussian states, for $N > 2$, is neither unbiased in the x_i and p_i quadratures (like the states discussed in Ref. [61] for $N = 3$), nor constructed by N equal squeezers ($r_m = r_p = \bar{r}$), as shown in Fig. 6(a). This latter case, which denotes exactly the states used to demonstrate a tripartite CV teleportation network experimentally [37], is clearly not optimal. In fact, it yields fidelities lower than $1/2$ for $N \geq 30$ and \bar{r} belonging to a certain interval [29]. A close analysis [36] shows that the problem does not lie in the choice of the protocol, but rather in the choice of the resource states. If the shared N -mode squeezed states are prepared (or transformed by local unitary operations) in the optimal form fulfilling Eq. (65), the teleportation fidelity \mathcal{F}^{opt} from Eq. (66) is guaranteed to be nonclassical as soon as $\bar{r} > 0$ for any N , in which case the considered class of pure states is genuinely multipartite entangled [29, 33, 30, 12, 16, 10], as we have mentioned in the previous sections. In fact, one can show that this nonclassical optimal fidelity is *necessary and sufficient* for the presence of multipartite entanglement in any multimode symmetric Gaussian state used as a shared resource for CV teleportation. This *equivalence*, stated in Ref. [36], silences the embarrassing question that entanglement might not be an actual physical resource, as protocols based on some entangled states might behave worse than their classical counterparts in processing quantum information.

For the quantification of multipartite entanglement, a crucial role is played by the quantity $\tilde{\nu}_-^{(N)}$, whose interpretation is clarified by the following argument. The considered teleportation network [29] is realized in two steps: first, the $N - 2$ cooperating parties perform local measurements on their modes, then Alice and Bob exploit their resulting entangled two-mode state to accomplish standard teleportation. The first stage of the process describes a concentration, or *localization*, of the original multipartite entanglement into bipartite entanglement between two modes [29, 33]. The maximum entanglement that one is able to concentrate in two parties, by performing local measurements on the other parties, is known as the *localizable entanglement* of a multipartite system [62, 63] (not to be confused with the *unitarily* localizable entanglement [10] discussed in Sec. 2.2, which is reversibly concentrated by unitary operations).[§] In our setting, the localizable entanglement is the

[§] Notice that such a nonunitary localization process, based on measurements and postselection, is a *probabilistic* procedure requiring many copy of the original state. On the other hand, the *deterministic* unitary localization requires only one copy of the state to be perfectly achieved.

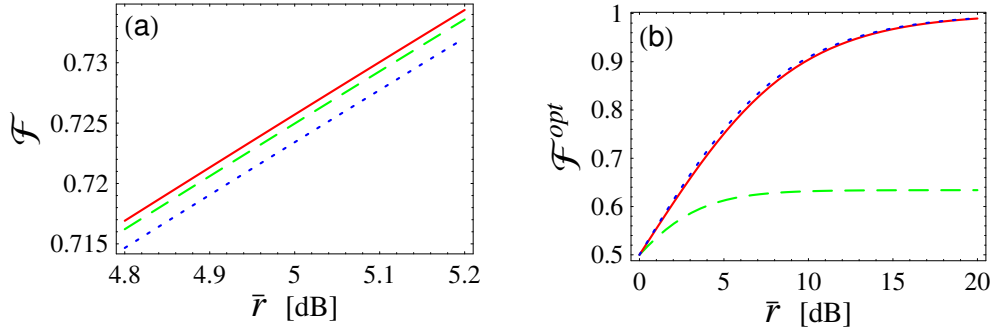


Figure 6. (a) Plot of the fidelities for teleporting an arbitrary coherent state from any sender to any receiver chosen from $N = 3$ parties, sharing a GHZ/W state. In a small window of average squeezing, we compare the optimal fidelity [36] (solid line), the fidelity obtained for the unbiased states discussed in Ref. [61] (dashed line), and the fidelity for states produced with all equal squeezers [29] (dotted line). The three curves are very close to each other, but the optimal preparation yields always the highest fidelity. (b) Expected success for an experimental test of the promiscuous sharing of CV entanglement in GHZ/W states. Referring to the check-list in Sec. 4.4: the solid curve realizes point (i), being the optimal fidelity \mathcal{F}_3^{opt} of a three-party teleportation network; the dotted curve realizes point (ii), being the optimal fidelity $\mathcal{F}_{2:uni}^{opt}$ of two-party teleportation exploiting the two-mode pure resource obtained from a unitary localization applied on two of the modes; the dashed curve realizes point (iii), being the optimal fidelity $\mathcal{F}_{2:red}^{opt}$ of two-party teleportation exploiting the two-mode mixed resource obtained discarding a mode. All of them lie above the classical threshold, providing a direct evidence of the promiscuity of entanglement sharing in the employed resources.

maximal entanglement that can be concentrated into two modes, by unitary operations and nonunitary momentum detections performed locally on the others. It turns out that the smallest symplectic eigenvalue (see Sec. 2.1) of the partial transpose of the resulting optimal two-mode state $\sigma_{loc}^{(N)}$, is exactly $\tilde{\nu}_-^{(N)}$ from Eq. (66) [36].

Eq. (66) thus relates two *operative* aspects of multipartite entanglement: the maximal fidelity achievable in a multi-user teleportation network [29] and the localizable entanglement [62]. These results yield quite naturally a direct operative way to quantify multipartite entanglement in N -mode (mixed) symmetric Gaussian states, in terms of the so-called *Entanglement of Teleportation* [36], defined as the normalized optimal fidelity

$$E_T^{(N)} \equiv \max \left\{ 0, \frac{\mathcal{F}_N^{opt} - \mathcal{F}_{cl}}{1 - \mathcal{F}_{cl}} \right\} = \max \left\{ 0, \frac{1 - \tilde{\nu}_-^{(N)}}{1 + \tilde{\nu}_-^{(N)}} \right\}, \quad (67)$$

and thus ranging from 0 (separable states) to 1 (infinitely squeezed CV GHZ/W states). The localizable entanglement (quantifiable by the negativity, the bipartite contangle, or the entanglement of formation) is a monotonically increasing function of E_T . For $N = 2$ the state is already localized and the optimal fidelity is a direct measure of entanglement in the shared two-mode resource. In the next subsection we will see how the entanglement of teleportation relates, for three-mode states, to the residual Gaussian contangle introduced in Sec. 3.2.

6.2. Testing the promiscuous sharing of tripartite entanglement

Let us focus, for the scope of the present section, on the case $N = 3$, *i.e.* on three-mode states shared as resources for a three-party teleportation network. This protocol is a basic, natural candidate to operationally investigate the sharing structure of CV entanglement in three-mode symmetric Gaussian states.

A first theoretical question that arises is to compare the tripartite entanglement of teleportation Eq. (67), which possesses a strong operational motivation, and the tripartite residual (Gaussian) contangle Eq. (13), which is built on solid mathematical foundations (being an entanglement monotone under GLOCC). Remarkably, in the case of pure three-mode shared resources [*i.e.* CV GHZ/W states, obtained by setting $n_m = n_p = 1$ in Eqs. (61,62)], *the two measures are completely equivalent*, being monotonically increasing functions of each other. Namely [36],

$$G_{\tau}^{res} = \log_2 \frac{2\sqrt{2}E_T - (E_T + 1)\sqrt{E_T^2 + 1}}{(E_T - 1)\sqrt{E_T(E_T + 4) + 1}} - \frac{1}{2} \log_2 \frac{E_T^2 + 1}{E_T(E_T + 4) + 1}, \quad (68)$$

where $E_T \equiv E_T^{(3)}$. Let us moreover recall that G_{τ}^{res} coincides with the true residual contangle in these states (see Sec. 4.2).

This fact entails that there is a ‘unique’ kind of three-party CV entanglement in pure *symmetric* three-mode Gaussian states, which merges at least three (usually inequivalent) properties: those of being maximally genuinely tripartite entangled, maximally bipartite entangled in any two-mode reduction, and ‘maximally efficient’ (in the sense of the optimal fidelity) for three-mode teleportation networks. Furthermore, this result paves the way towards an experimental test for the promiscuous sharing of CV entanglement in symmetric Gaussian states. To unveil this peculiar feature, one should prepare a CV GHZ/W state in the optimal form, given by Eq. (65). It is worth remarking that, in the case of three modes, non-optimal forms like that produced with $r_m = r_p$ [18, 37] yield fidelities really close to the maximal one [see Fig. 6(a)], and are thus practically as good as the optimal states (if not even better, taking into account that the states with $r_m = r_p$ are generally easier to produce in practice).

To detect the presence of tripartite entanglement, one should be able to implement the network in at least two different combinations [37], so that the teleportation would be accomplished, for instance, from mode 1 to mode 2 with the assistance of mode 3, and from mode 2 to mode 3 with the assistance of mode 1. To be complete (even if it is not strictly needed [12]), one could also realize the transfer from mode 3 to mode 1 with the assistance of mode 2. Taking into account a realistic asymmetry among the modes, the average experimental fidelity \mathcal{F}_3^{opt} over the three possible situations would provide a direct quantitative measure of tripartite entanglement, through Eqs. (66–68).

To demonstrate the promiscuous sharing, one would then need to discard each one of the modes at a time, and perform standard two-user teleportation between the remaining pair of parties. The optimal fidelity for this two-user teleportation (obtained exactly for $r_m = r_p$) is

$$\mathcal{F}_{2:red}^{opt} = \frac{3}{3 + \sqrt{3 + 6e^{-4\bar{r}}}}. \quad (69)$$

Again, one should implement the three possible configurations and take the average fidelity as figure of merit. As anticipated in 4.4, this fidelity cannot reach unity because the entanglement in the shared mixed resource remains finite, and in fact $\mathcal{F}_{2:red}^{opt}$ saturates to $3/(3 + \sqrt{3}) \approx 0.634$ in the limit of infinite squeezing.

Finding simultaneously both \mathcal{F}_3^{opt} and $\mathcal{F}_{2:red}^{opt}$ above the classical threshold Eq. (58), at fixed squeezing \bar{r} , would be a clear experimental fingerprint of the promiscuous sharing of CV entanglement. Theoretically, this is true for all $\bar{r} > 0$, as shown in Fig. 6(b). From an experimental point of view, the tripartite teleportation network has been recently implemented, and the genuine tripartite shared entanglement unambiguously demonstrated by obtaining a nonclassical teleportation fidelity (up to 0.64 ± 0.02) in all the three possible user configurations [37]. Nevertheless, a nonclassical fidelity $\mathcal{F}_{2:red}$ in the teleportation exploiting

any two-mode reduction was not observed. This fact can be consistently explained by taking into account experimental noise. In fact, even if the desired resource states were pure GHZ/W states, the unavoidable effects of decoherence and imperfections resulted in the experimental production of *mixed* states, namely of the noisy GHZ/W states discussed in Sec. 4.5. It is very likely that the noise was too high compared with the pumped squeezing, so that the actual produced states were still fully inseparable, but laid outside the region of promiscuous sharing (see Fig. 5), having no entanglement left in the two-mode reductions. However, increasing the degree of initial squeezing, and/or reducing the noise sources might be accomplished with the state-of-the-art equipment employed in the experiments of Ref. [37] (see also [57]). The conditions required for a proper test (to be followed by actual practical applications) of the promiscuous sharing of CV entanglement in symmetric three-mode Gaussian states, as detailed in Sec. 4.4, should be thus met shortly. As a final remark, let us observe that repeating the same experiment but employing T states, introduced in Sec. 4.3, as resources, would be another interesting option. In fact, in this case the expected optimal fidelity is strictly smaller than in the case of GHZ/W states, confirming the promiscuous structure in which the reduced bipartite entanglement enhances the value of the genuine tripartite one.

With the same GHZ/W shared resources (but also with all symmetric and bisymmetric three-mode Gaussian states, including T states, noisy GHZ/W states and basset-hound states), one may also test the power of the unitary localization of entanglement [10] (Sec. 2.2), as opposed to the nonunitary localization of entanglement by measurements [62, 63], needed for the teleportation network. Suppose that the three parties Alice, Bob and Claire share a GHZ/W state. If Bob and Claire are allowed to cooperate (nonlocally), they can combine their respective modes at a 50:50 beam splitter. The result is an entangled state shared by Alice and Bob, while Claire is left with an uncorrelated state. The optimal fidelity of standard teleportation from Alice to Bob with the unitarily localized resource, reads

$$\mathcal{F}_{2:uni}^{opt} = \left[\frac{1}{3} \left(\sqrt{4 \cosh(4\bar{r}) + 5} - 2\sqrt{\cosh(4\bar{r}) - 1} \right) + 1 \right]^{-1}. \quad (70)$$

Notice that $\mathcal{F}_{2:uni}^{opt}$ is larger than \mathcal{F}_3^{opt} [see Fig. 6(b)]. This is true for any number N of modes, and the difference between the two, at fixed squeezing, increases with N , confirming that the unitarily localizable entanglement of [10] is strictly stronger than the (nonunitarily) localizable entanglement of Refs. [62, 63], as discussed in Ref. [31]. This is of course not surprising, as the unitary localization generally requires a high degree of nonlocal control on the two subset of modes, while the localizable entanglement is defined in terms of LOCC alone.

Throughout this whole subsection, we have only dealt with completely symmetric resource states, due to the invariance requirements of the considered protocol. In Ref. [36], the question whether expressions like Eq. (66) and Eq. (67), connecting the optimal fidelity and the entanglement of teleportation to the symplectic eigenvalue $\tilde{\nu}_-^{(N)}$, hold as well for nonsymmetric entangled resources, was left open (see also Ref. [53]). In Sec. 7, devoted to telecloning, we will show with a specific counterexample that this is *not* the case, not even in the simplest case of $N = 2$.

6.3. Degradation of teleportation efficiency under quantum noise

In Ref. [2] we have addressed the decay of three-partite entanglement (as quantified by the residual Gaussian contangle) of three-mode states in the presence of losses and thermal noise. We aim now at relating such an ‘abstract’ analysis to precise operational statements, by investigating the decay of the optimal teleportation fidelity of shared three-mode resources

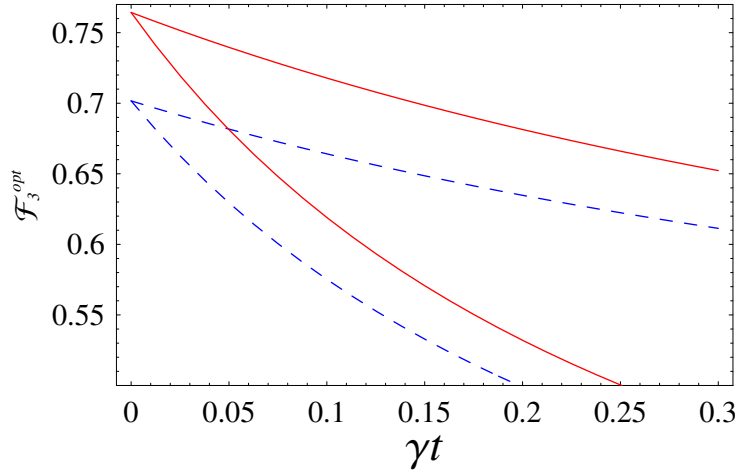


Figure 7. Evolution of the optimal fidelity \mathcal{F}_3^{opt} for GHZ/W states with local mixedness $a = 2$ (corresponding to $\bar{r} \simeq 0.6842$) (solid lines) and T states with local mixedness $a = 2.8014$. Such states have equal initial residual contangle. Uppermost curves refer to baths with $n = 0$ ('pure losses'), while lowermost curves refer to baths with $n = 1$. T states affording for the same initial fidelity as the considered GHZ/W state were also considered, and found to degrade faster than the GHZ/W state.

subject to environmental decoherence. This study will also provide further heuristic justification for the residual contangle as a proper measure of tripartite entanglement even for mixed ('decohered') Gaussian states. Notice that the effect of decoherence occurring *during* the creation of the state on the teleportation fidelity has been already implicitly considered in Eq. 66, by the noise terms n_m and n_p . Here, we will instead focus on the decay of the teleportation efficiency under decoherence affecting the resource states *after* their distribution to the distant parties.

We will assume, realistically, a local decoherence (*i.e.* with no correlated noises) for the three modes, in thermal baths with equal average photon number n . The evolving states maintain their Gaussian character under such evolution (for a detailed description of the master equation governing the system and of its Gaussian solutions, refer to [2]).

As initial resources, we have considered both pure GHZ/W states and mixed T states, described in Sec. 4.3. The results, showing the exact evolution of the fidelity \mathcal{F}_3^{opt} (optimized over local unitaries) of teleportation networks exploiting such initial states, are shown in Fig. 7. GHZ/W states, already introduced as "optimal" resources for teleportation networks, were also found to allow for protocols most robust under decoherence. Notice how the qualitative behaviour of the curves of Fig. 7 follow that of Fig. 5 of Ref. [2], where the evolution of the residual Gaussian contangle of the same states under the same conditions is plotted. Also the vanishing of entanglement at finite times (occurring only in the presence of thermal photons, *i.e.* for $n > 0$) reciprocates the fall of the fidelity below the classical threshold of $1/2$. The status of the residual contangle as a measure reflecting operational aspects of the states is thus strengthened in this respect, even in the region of mixed states. Notice, though, that Fig. 7 also confirms that, as already stated, the entanglement of teleportation is not equivalent to the residual Gaussian contangle, as the initial GHZ/W and T states of Fig. 7 have the same initial residual Gaussian contangle but grant manifestly different fidelities and, further, the times at which the classical threshold is trespassed do not exactly coincide with the times at which the residual contangle vanishes.

7. 1 → 2 telecloning with bisymmetric and nonsymmetric resources

Quantum *telecloning* [64] among $N + 1$ parties is defined as a process in which one party (Alice) owns an unknown quantum state, and wants to distribute her state, via teleportation, to all the other N remote parties. The no-cloning theorem [65, 66] yields that the $N - 1$ remote clones can resemble the original input state only with a finite, nonmaximal fidelity. In CV systems, $1 \rightarrow N$ telecloning of arbitrary coherent states was proposed in Ref. [48], involving a special class of $(N + 1)$ -mode multiparty entangled Gaussian states (known as “multiuser quantum channels”) shared as resources among the $N + 1$ users. The telecloning is then realized by a succession of standard two-party teleportations between the sender Alice and each of the N remote receivers, exploiting each time the corresponding reduced two-mode state shared by the selected pair of parties.

Depending on the symmetries of the shared resource, the telecloning can be realized with equal fidelities for all receivers (*symmetric* telecloning) or with unbalanced fidelities among the different receivers (*asymmetric* telecloning). In particular, in the first case, the needed resource must have complete invariance under mode permutations in the N -mode block distributed among the receivers: the resource state has to be thus a $1 \times N$ bisymmetric state [16, 10] (see Fig. 1).

In this manuscript we specialize on $1 \rightarrow 2$ telecloning, where Alice, Bob and Claire share a tripartite entangled three-mode Gaussian state and Alice wants to teleport arbitrary coherent states to Bob and Claire with certain fidelities. As the process itself suggests, the crucial resource enabling telecloning is not the genuine tripartite entanglement (needed instead for a successful ‘multidirectional’ teleportation network, as shown in the previous section), but the couplewise entanglement between the pair of modes $1|2$ and $1|3$ [if the sender (Alice) owns mode 1, while the receivers (Bob and Claire) own modes 2 and 3].

7.1. Symmetric telecloning

Let us first analyze the case of symmetric telecloning, occurring when Alice aims at sending two copies of the original state with equal fidelities to Bob and Claire. In this case it has been proven [67, 68, 48] that Alice can teleport an arbitrary coherent state to the two distant twins Bob and Claire (employing a Gaussian cloning machine) with the maximal fidelity

$$\mathcal{F}_{\max}^{1 \rightarrow 2} = \frac{2}{3}. \quad (71)$$

This argument inspired the introduction of the ‘no-cloning threshold’ for two-party teleportation was established [69], basically stating that only a fidelity greater than $2/3$ (thus greater than the previously introduced threshold of $1/2$, which implies the presence of entanglement) ensures the realization of actual two-party quantum teleportation of a coherent state. In fact, if the fidelity falls in the range $1/2 < \mathcal{F} < 2/3$, then Alice could have kept a better copy of the input state for herself, or sent it to a ‘malicious’ Claire. In this latter case, the whole process would result into an asymmetric telecloning, with a fidelity $\mathcal{F} > 2/3$ for the copy received by Claire. It is worth remarking that, as already mentioned, two-party CV teleportation beyond the no-cloning threshold has been recently demonstrated experimentally, with a fidelity $\mathcal{F} = 0.70 \pm 0.02$ [57]. Another important and surprising remark is that the fidelity of $1 \rightarrow 2$ cloning of coherent states, given by Eq. (71), is *not* the optimal one. As recently shown in Ref. [70], using non-Gaussian operations as well, two identical copies of an arbitrary coherent state can be obtained with optimal single-clone fidelity $\mathcal{F} \approx 0.6826$.

In our setting, dealing with three-mode Gaussian states and Gaussian operations only, the basset-hound states σ_B^p of Sec. 4.6 are, as previously anticipated, the best suited resource

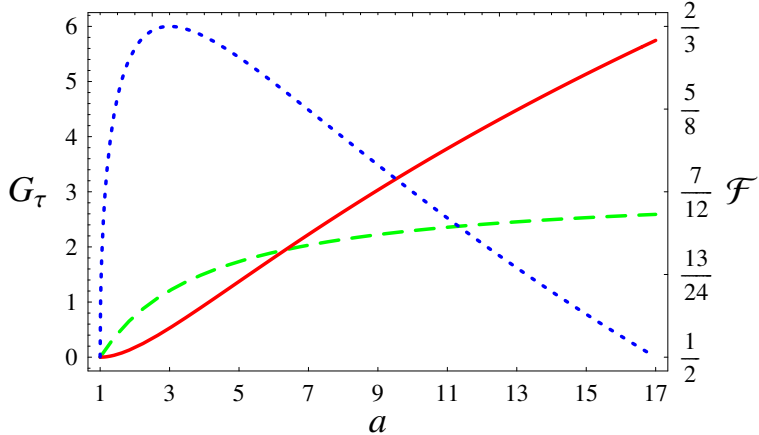


Figure 8. Bipartite entanglement $G_\tau^{1|l}$ (dashed line) in $1|l$ ($l = 2, 3$) two-mode reductions of basset-hound states, and genuine tripartite entanglement G_τ^{res} (solid line) among the three modes, versus the local mixedness a of mode 1. Entanglements are quantified by the Gaussian contangle. The fidelity $\mathcal{F}_{sym}^{1 \rightarrow 2}$ of symmetric $1 \rightarrow 2$ telecloning employing basset-hound resource states is plotted as well (dotted line, scaled on the right axis), reaching its optimal value of $2/3$ for $a = 3$.

states for symmetric telecloning. Such states belong to the family of multiuser quantum channels introduced in Ref. [48], and are 1×2 bisymmetric pure states, parametrized by the single-mode mixedness a of mode 1. In particular, it is interesting to study how the single-clone telecloning fidelity behaves compared with the actual amount of entanglement in the $1|l$ ($l = 2, 3$) nonsymmetric two-mode reductions of σ_B^p states.

A brief excursus has to be made here. Setting, as usual, all first moments to zero, the fidelity of two-user teleportation of arbitrary single-mode Gaussian states exploiting two-mode Gaussian resources can be computed directly from the respective CMs [71]. Being σ_{in} the CM of the unknown input state, and

$$\sigma_{ab} = \begin{pmatrix} \sigma_a & \varepsilon_{ab} \\ \varepsilon_{ab}^\top & \sigma_b \end{pmatrix}, \quad (72)$$

the CM of the shared two-mode resource, and defining the matrix $\xi = \text{diag}\{-1, 1\}$, the fidelity reads [71]

$$\mathcal{F} = \frac{2}{\sqrt{\text{Det } \Sigma}}, \quad \Sigma \equiv 2\sigma_{in} + \xi\sigma_a\xi + \sigma_b + \xi\varepsilon_{ab} + \varepsilon_{ab}^\top\xi. \quad (73)$$

In our case, $\sigma_{in} = \mathbb{1}_2$ because Alice is teleporting coherent states, while the resource σ_{ab} is obtained discarding either the third ($a = 1, b = 2$) or the second ($a = 1, b = 3$) mode from the CM σ_B^p of basset-hound states. From Eqs. (49, 50, 73), the single-clone fidelity for symmetric $1 \rightarrow 2$ telecloning exploiting basset-hound states is:

$$\mathcal{F}_{sym}^{1 \rightarrow 2} = \frac{4}{3a - 2\sqrt{2}\sqrt{a^2 - 1} + 5}. \quad (74)$$

Notice, remembering that each of modes 2 and 3 contains an average number of photons $\bar{n} = (a - 1)/2$, that Eq. (74) is the same as Eq. (19) of Ref. [43], where a production scheme for three-mode Gaussian states by interlinked nonlinear interactions in $\chi^{(2)}$ media is presented, and the usefulness of the produced resources for $1 \rightarrow 2$ telecloning is discussed as

well. The basset-hound states realize an optimal symmetric cloning machine, *i.e.* the fidelity of both clones saturates Eq. (71), for the finite value $a = 3$. Surprisingly, with increasing $a > 3$, the fidelity Eq. (74) starts decreasing, even if the two-mode entanglements Eq. (53) in the reduced (nonsymmetric) bipartitions of modes $1|2$ and $1|3$, as well as the genuine tripartite entanglement Eq. (51), increase with increasing a . As shown in Fig. 8, the telecloning fidelity is not a monotonic function of the employed bipartite entanglement. Rather, it roughly follows the difference $G_{\tau}^{1|l} - G_{\tau}^{res}$, being maximized where the bipartite entanglement is stronger than the tripartite one. This fact heuristically confirms that in basset-hound states bipartite and tripartite entanglements are competitors, meaning that the CV entanglement sharing in these states is not promiscuous, as described in Sec. 4.6.

The example of basset-hound states represents a clear hint that the teleportation fidelity with generic two-mode (pure or mixed) nonsymmetric resources is *not* monotone with the entanglement. Even if an hypothetical optimization of the fidelity over the local unitary operations could be performed (on the guidelines of [36]), it would entail a fidelity growing up to $2/3$ and then staying constant while entanglement increases, which means that no direct estimation of the entanglement can be extracted from the nonsymmetric teleportation fidelity, at variance with the symmetric case (see the previous section). To exhibit a quantitative argument, suppose that Eq. (66) (with $N = 2$) held for nonsymmetric resources as well. Applying it to the $1|l$ ($l = 2, 3$) two-mode reduced resources obtained from basset-hound states, would imply an “optimal” fidelity reaching $3/4$ in the limit $a \rightarrow \infty$. But this value is impossible to achieve, even considering non-Gaussian cloning machines [70]: thus, the simple relation between teleportation fidelity and entanglement, formalized by Eq. (66), fails to hold for nonsymmetric resources, even in the basic two-mode instance.

This somewhat controversial result can be to some extent interpreted as follows. For symmetric Gaussian states, there exists a ‘unique type’ of bipartite CV entanglement. In fact, measures such as the logarithmic negativity (quantifying the violation of the mathematical PPT criterion), the entanglement of formation (related to the entanglement cost, and thus quantifying how expensive is the process of creating a mixed entangled state through LOCC), and the degree of EPR correlation (quantifying the correlations between the entangled degrees of freedom) are *all* completely equivalent for such states, being monotonic functions of only the smallest symplectic eigenvalue $\tilde{\nu}_-$ of the partially transposed CM. As we have seen, this equivalence extends also to the efficiency of two-user quantum teleportation, quantified by the fidelity optimized over local unitaries. For nonsymmetric states, the chain of equivalences breaks down. In hindsight, this could have been somehow expected, as there exist several inequivalent but legitimate measures of entanglement, each of them capturing distinct aspects of the quantum correlations. In the specific instance of nonsymmetric two-mode Gaussian states, it has been shown that the negativity is neither equivalent to the (Gaussian) entanglement of formation (the two measures may induce inverted orderings on this subset of entangled states) [46], nor to the EPR correlation [45]. It is thus justified that a process like teleportation emphasizes a distinct aspect of the entanglement encoded in nonsymmetric resources. Notice also that the richer and more complex entanglement structure of non symmetric states, as compared to that of symmetric states, reflects a crucial operational difference in the respective (asymmetric and symmetric) teleportation protocols. While in the symmetric protocols the choice of sender and receiver obviously does not affect the fidelity, this is no longer the case in the asymmetric instance: this physical asymmetry between sender and receiver properly exemplifies the more complex nature of the two-mode asymmetric entanglement.

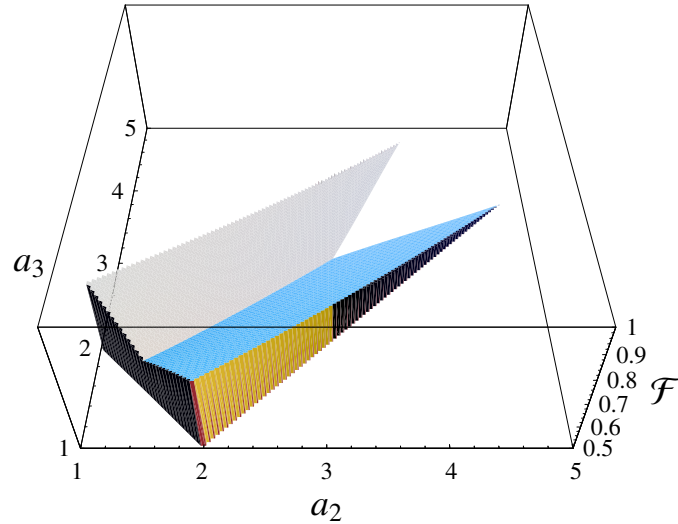


Figure 9. Fidelities for asymmetric telecloning with three-mode pure Gaussian resources, at a fixed $a_1 = 2$, as functions of a_2 and a_3 , varying in the allowed range of parameters constrained by Ineq. (5) (see also Fig. 3). The darker surface on the right-hand side of the diagonal $a_2 = a_3$ (along which the two surfaces intersect) is the fidelity of Bob's clone, $\mathcal{F}_{asym:2}^{1\rightarrow 2}$, while the lighter, ‘mirror-reflected’ surface on the left-hand side of the diagonal is the fidelity of Claire's clone, $\mathcal{F}_{asym:3}^{1\rightarrow 2}$. Only nonclassical fidelities (*i.e.* $\mathcal{F} > 1/2$) are shown.

7.2. Asymmetric telecloning

In this section we focus on the *asymmetric* telecloning of coherent states, through generic pure three-mode Gaussian states shared as resources among the three parties. Considering states in standard form (see Sec. 2.2 and Ref. [2]), parametrized by the local single-mode mixednesses a_i of modes $i = 1, 2, 3$, the fidelity $\mathcal{F}_{asym:2}^{1\rightarrow 2}$ of Bob's clone (employing the $1|2$ two-mode reduced resource) can be computed from Eq. (73) and reads

$$\begin{aligned} \mathcal{F}_{asym:2}^{1\rightarrow 2} = 2 \left\{ & -2a_3^2 + 2a_1a_2 + 4(a_1 + a_2) + 3(a_1^2 + a_2^2) \right. \\ & \left. - (a_1 + a_2 + 2) \sqrt{\frac{[(a_1 + a_2 - a_3)^2 - 1][(a_1 + a_2 + a_3)^2 - 1]}{a_1a_2}} + 2 \right\}^{-\frac{1}{2}}, \end{aligned} \quad (75)$$

Similarly, the fidelity $\mathcal{F}_{asym:3}^{1\rightarrow 2}$ of Claire's clone can be obtained from Eq. (75) by exchanging the roles of “2” and “3”.

It is of great interest to explore the space of parameters $\{a_1, a_2, a_3\}$ in order to find out which three-mode states allow for an asymmetric telecloning with the fidelity of one clone above the symmetric threshold of $2/3$, while keeping the fidelity of the other clone above the classical threshold of $1/2$. Let us keep a_1 fixed. With increasing difference between a_2 and a_3 , one of the two telecloning fidelities increases at the detriment of the other, while with increasing sum $a_2 + a_3$ both fidelities decrease to fall eventually below the classical threshold, as shown in Fig. 9. The asymmetric telecloning is thus *optimal* when the sum of the two local mixednesses of modes 2 and 3 saturates its lower bound. From Ineq. (5), the optimal resources must have

$$a_3 = a_1 - a_2 + 1, \quad (76)$$

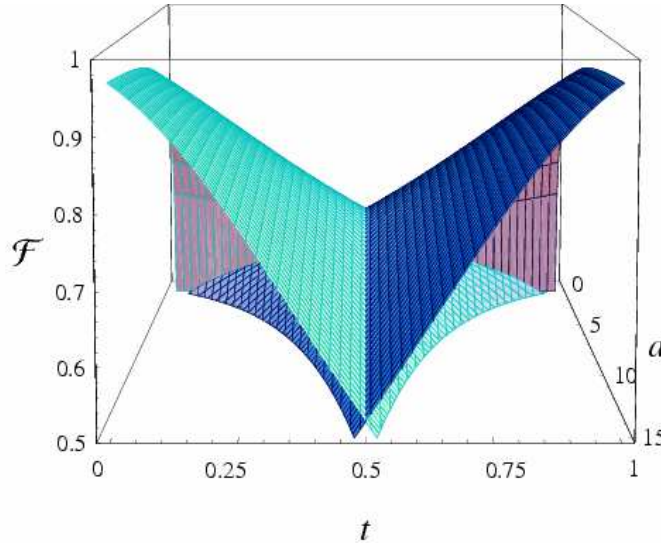


Figure 10. Optimal fidelities for asymmetric telecloning with three-mode pure Gaussian resources, as functions of the single-mode mixedness a of mode 1, and of the parameter t determining the local mixednesses of the other modes, through Eqs. (76,77). The darker, rightmost surface is the optimal fidelity of Bob's clone, $\mathcal{F}_{asym:2}^{opt:1\rightarrow 2}$, while the lighter, leftmost surface is the optimal fidelity of Claire's clone, $\mathcal{F}_{asym:3}^{opt:1\rightarrow 2}$. Along the intersection line $t = 1/2$ the telecloning is symmetric. Only nonclassical fidelities (i.e. $\mathcal{F} > 1/2$) are shown.

A suitable parametrization of these states is obtained setting $a_1 \equiv a$ and

$$a_2 = 1 + (a - 1)t, \quad 0 \leq t \leq 1. \quad (77)$$

For $t < 1/2$ the fidelity of Bob's clone is smaller than that of Claire's one, $\mathcal{F}_{asym:2}^{1\rightarrow 2} < \mathcal{F}_{asym:3}^{1\rightarrow 2}$, while for $t > 1/2$ the situation is reversed. In all the subsequent discussion, notice that Bob and Claire swap their roles if t is replaced by $1 - t$. For $t = 1/2$, the asymmetric resources reduce to the bisymmetric basset-hound states useful for symmetric telecloning. The optimal telecloning fidelities then read

$$\mathcal{F}_{asym:2}^{opt:1\rightarrow 2} = \frac{2}{\sqrt{(a+3)^2 + (a-1)^2 t^2 + 2(a-1)(3a+5)t - 4\sqrt{(a^2-1)t}a + (a-1)t + 3}}, \quad (78)$$

and similarly for $\mathcal{F}_{asym:3}^{opt:1\rightarrow 2}$ replacing t by $1 - t$. The two optimal fidelities are plotted in Fig. 10

With these pure nonsymmetric resources, further optimizations can be performed depending on the needed task. For instance, one may need to implement telecloning with the highest possible fidelity of one clone, while keeping the other nonclassical. This problem is of straightforward solution, and yields optimal asymmetric resources with

$$a = \frac{7}{2}, \quad t = \frac{4}{5}. \quad (79)$$

In this case the fidelity of Claire's clone saturates the classical threshold, $\mathcal{F}_{asym:3}^{opt:1\rightarrow 2} = 1/2$, while the fidelity of Bob's clone reaches $\mathcal{F}_{asym:2}^{opt:1\rightarrow 2} = 4/5$, which is the maximum allowed value for this setting [72]. Also, choosing $t = 1/5$, Bob's fidelity gets classical and Claire's fidelity is maximal.

In general, a telecloning with $\mathcal{F}_{asym:2}^{opt:1\rightarrow 2} \geq 2/3$ and $\mathcal{F}_{asym:3}^{opt:1\rightarrow 2} \geq 1/2$ is possible only in the window

$$1.26 \approx 2\sqrt{2} \left[2 - \sqrt{1 + \sqrt{2}} \right] \leq a \leq 2\sqrt{2} \left[2 + \sqrt{1 + \sqrt{2}} \right] \approx 10.05 \quad (80)$$

and, for each a falling in the region defined by Ineq. (80), in the specific range

$$\frac{a - 2\sqrt{a + 1} + 2}{a - 1} \leq t \leq \frac{2(\sqrt{2}\sqrt{a + 1} - 2)}{a - 1}. \quad (81)$$

For instance, for $a = 3$, the optimal asymmetric telecloning (with Bob's fidelity above no-cloning and Claire's fidelity above classical bound) is possible in the whole range $1/2 \leq t \leq 2\sqrt{2} - 1$, where the boundary $t = 1/2$ denotes the basset-hound state realizing optimal symmetric telecloning (see Fig. 8). The sum $\mathcal{S}^{opt:1\rightarrow 2} = \mathcal{F}_{asym:2}^{opt:1\rightarrow 2} + \mathcal{F}_{asym:3}^{opt:1\rightarrow 2}$ can be maximized as well, and the optimization is realized by values of a falling in the range $2.36 \lesssim a \leq 3$, depending on t . The absolute maximum of $\mathcal{S}^{opt:1\rightarrow 2}$ is reached, as expected, in the fully symmetric instance $t = 1/2$, $a = 3$, and yields $\mathcal{S}_{\max}^{opt:1\rightarrow 2} = 4/3$.

We finally recall that optimal three-mode Gaussian resources, can be produced by implementing the allotment operator (see Sec. 4.1), and employed to perform all-optical symmetric and asymmetric telecloning machines [48, 72].

8. Conclusions

In the present paper and in Ref. [2], we have aimed at providing a (to a good extent) comprehensive treatment on the characterization, quantification and experimental generation of genuine multipartite entanglement in three-mode Gaussian states of CV systems, including relevant, practical implementations in the context of CV quantum information.

Similarly with what happens for bipartite entanglement in symmetric Gaussian states, but at striking variance with the discrete-variable scenario (in particular for systems of three qubits), we have shown that there is a *unique* kind of genuine tripartite entanglement in pure, symmetric, three-mode Gaussian states, which combines a mathematical significance in the context of entanglement sharing with an operational interpretation in terms of teleportation experiments. This fact is a remarkable consequence of the restriction to Gaussian states, as the proven existence, for infinite dimensional systems, of infinitely many mutually stochastic-LOCC-incomparable states (even under the bounded energy and finite information exchange condition) suggests [73]. Even more strikingly, this tripartite entanglement distributes in a *promiscuous* way, being enhanced by the presence of bipartite entanglement in any two-mode reduction. Here we have shown that the promiscuity of CV entanglement survives even for non-pure states like noisy GHZ/W states, with purities down to 0.2. However, with increasing mixedness the structure of three-party entanglement enriches, as tripartite bound entangled states can exist even in the fully symmetric instance. For nonsymmetric (pure or mixed) three-mode states, the promiscuity fades leaving room for a more traditional entanglement sharing structure. We further remark that for all fully inseparable Gaussian states (which represent one of the five possible separability classes [1]), the residual Gaussian contangle, or *arravagliament*, is a *bona fide*, computable measure of genuine tripartite entanglement, as first proven in Ref. [15] and presented in full detail in Ref. [2].

The core of this paper has been devoted to providing several examples of tripartite entangled Gaussian states, relevant for their entanglement properties and/or for applications in CV quantum information. For each of them, we have computed the tripartite entanglement explicitly, and dedicated great attention to quantum state engineering, proposing schemes

for the experimental production of the considered states. In particular we developed a self-contained procedure to engineer arbitrary pure three-mode Gaussian states by means of linear optics, based on the distribution, or *allotment* of two-mode entanglement among three modes.

In the last part of this work we have investigated the potentialities of the introduced families of three-mode Gaussian states for the implementation of multipartite quantum communication protocols with continuous variables. This has allowed us to focus on the physical significance of the applied ‘genuine multipartite’ entanglement measure (arravogliament), shifting the analysis’s testing ground from the domain of mathematical convenience to that of operational effectiveness.

Acknowledgments

Financial support from MIUR, INFN, and CNR is acknowledged. G A is grateful to Samanta Piano for her encouraging advice, and for reminding him of the sentence quoted in the caption of Fig. 1. A S is currently a Marie Curie fellow at Imperial College London; he also acknowledges EPSRC for financial support (through the QIP-IRC) and the Centre for Mathematical Sciences of the University of Cambridge for kind hospitality.

References

- [1] Giedke G, Kraus B, Lewenstein M and Cirac J I 2001 *Phys. Rev. Lett.* **64** 052313
- [2] Adesso G, Serafini A and Illuminati F 2006 *Phys. Rev. A* **73** 032345
- [3] Braunstein S L and Pati A K (eds) 2003 *Quantum Information Theory with Continuous Variables* (Dordrecht: Kluwer Academic Publishers)
- [4] Cerf N, Leuchs G and Polzik E S (eds) 2006 in press *Quantum Information with Continuous Variables of Atoms and Light* (London: Imperial College Press)
- [5] Braunstein S L and van Loock P 2005 *Rev. Mod. Phys.* **77** 513
- [6] Simon R, Sudarshan E C G and Mukunda N 1987 *Phys. Rev. A* **36** 3868
- [7] Simon R 2000 *Phys. Rev. Lett.* **84** 2726
- [8] Duan L-M, Giedke G, Cirac J I and Zoller P 2000 *Phys. Rev. Lett.* **84** 2722
- [9] Werner R F and Wolf M M 2001 *Phys. Rev. Lett.* **86** 3658
- [10] Serafini A, Adesso G and Illuminati F 2005 *Phys. Rev. A* **71** 032349
- [11] Vidal G and Werner R F 2002 *Phys. Rev. A* **65** 032314
- [12] van Loock P and Furusawa A 2003 *Phys. Rev. A* **67** 052315
- [13] Hyllus P and Eisert J 2006 *New J. Phys.* **8** 51
- [14] Paris M G A, Illuminati F, Serafini A and De Siena S 2003 *Phys. Rev. A* **68** 012314
- [15] Adesso G and Illuminati F 2006 *New J. Phys.* **8** 15
- [16] Adesso G, Serafini A and Illuminati F 2004 *Phys. Rev. Lett.* **93** 220504
- [17] Illuminati F 2001 public lecture. NO ANIMALS WERE HARMED IN THE MAKING OF FIGURE 1.
- [18] Aoki T, Takei N, Yonezawa H, Wakui K, Hiraoka T, Furusawa A and van Loock P 2003 *Phys. Rev. Lett.* **91** 080404
- [19] Bradley A S, Olsen M K, Pfister O and Pooser R C 2005 *Phys. Rev. A* **72** 053805
- [20] Hiroshima T, Adesso G and Illuminati F 2006 *Preprint* quant-ph/0605021
- [21] Coffman V, Kundu J and Wootters W K 2000 *Phys. Rev. A* **61** 052306
- [22] Osborne T J and Verstraete F 2006 *Phys. Rev. Lett.* **96** 220503
- [23] Giedke G, Wolf M M, Krüger O, Werner R F and Cirac J I 2003 *Phys. Rev. Lett.* **91** 107901
- [24] Krüger and Werner R F (eds) 2005 *Preprint* quant-ph/0504166 and
<http://www.imaph.tu-bs.de/qi/problems>
- [25] Wolf M M, Giedke G, Krüger O, Werner R F and Cirac J I 2004 *Phys. Rev. A* **69** 052320
- [26] Adesso G and Illuminati F 2006 *Int. J. Quant. Inf.* **4** 383
- [27] Arvind, Dutta B, Mukunda N and Simon R 1995 *Pramana* **45** 471, *Preprint* quant-ph/9509002
- [28] Laurat J, Keller G, Oliveira-Huguenin J A, Fabre C, Coudreau T, Serafini A, Adesso G and Illuminati F 2005 *J. Opt. B* **7** S577
- [29] van Loock P and Braunstein S L 2000 *Phys. Rev. Lett.* **84** 3482
- [30] van Loock P and Braunstein S L *Multipartite entanglement* in [3]

- [31] Adesso G and Illuminati F *Bipartite and Multipartite Entanglement of Gaussian States* in [4], *Preprint* quant-ph/0510052
- [32] van Loock P and Braunstein S L 2001 *Phys. Rev. A* **63** 022106
- [33] van Loock P 2002 *Fortschr. Phys.* **50** 1177
- [34] For a review on multiphoton state engineering see Dell'Anno F, De Siena S and Illuminati F 2006 *Phys. Rep.* **428** 53
- [35] Braunstein S L 1998 *Nature* **394** 47
- [36] Adesso G and Illuminati F 2005 *Phys. Rev. Lett.* **95** 150503
- [37] Yonezawa H, Aoki T and Furusawa A 2004 *Nature* **431** 430
- [38] Lance A M, Symul T, Bowen W P, Sanders B C and Lam P K 2004 *Phys. Rev. Lett.* **92** 177903
- [39] Jing J, Zhang J, Yan Y, Zhao F, Xie C and Peng K 2003 *Phys. Rev. Lett.* **90** 167903
- [40] Neegovzen R and Sanpera A 2005 *Preprint* quant-ph/0507249
- [41] Chen X-Y 2005 *Phys. Lett. A* **335** 121
- [42] Pirandola S, Mancini S, Vitali D and Tombesi P 2003 *Phys. Rev. A* **68** 062317
- [43] Ferraro A and Paris M G A 2005 *Phys. Rev. A* **72** 032312
- [44] Adesso G, Serafini A and Illuminati F 2004 *Phys. Rev. Lett.* **92** 087901
- [45] Adesso G, Serafini A and Illuminati F 2004 *Phys. Rev. A* **70** 022318
- [46] Adesso G and Illuminati F 2005 *Phys. Rev. A* **72** 032334
- [47] A generic covariance matrix element λ (denoting e.g. squeezing or noise) can be expressed in decibels (dB) via the formula $\lambda_{\text{dB}} = 10 \log_{10} \lambda$.
- [48] van Loock P and Braunstein S L 2001 *Phys. Rev. Lett.* **87** 247901
- [49] Wolf M M, Verstraete F and Cirac J I 2004 *Phys. Rev. Lett.* **93** 087903
- [50] Bennett C H, Brassard G, Crépeau C, Jozsa R, Peres A and Wootters W K 1993 *Phys. Rev. Lett.* **70** 1895
- [51] Bouwmeester D, Pan J-W, Mattle K, Eibl M, Weinfurter H and Zeilinger A 1997 *Nature* **390** 575
- [52] Boschi D, Branca S, De Martini F, Hardy L and Popescu S 1998 *Phys. Rev. Lett.* **80** 1121
- [53] Pirandola S and Mancini S 2006 *Preprint* quant-ph/0604027
- [54] Vaidman L 1994 *Phys. Rev. A* **49** 1473
- [55] Braunstein S L and Kimble H J 1998 *Phys. Rev. Lett.* **80** 869
- [56] Furusawa A, Sørensen J L, Braunstein S L, Fuchs C A, Kimble H J and Polzik E S 1998 *Science* **282** 706 (1998)
- [57] Takei N, Yonezawa H, Aoki T and Furusawa A 2005 *Phys. Rev. Lett.* **94** 220502
- [58] Braunstein S L, Fuchs C A and Kimble H J 2000 *J. Mod. Opt.* **47** 267
- [59] Hammerer K, Wolf M M, Polzik E S and Cirac J I 2005 *Phys. Rev. Lett.* **94** 150503
- [60] Pirandola S 2005 *Int. J. Quant. Inf.* **3** 239
- [61] Bowen W P, Lam P K and Ralph T C 2003 *J. Mod. Opt.* **50** 801
- [62] Verstraete F, Popp M, and Cirac J I 2004 *Phys. Rev. Lett.* **92** 027901
- [63] Popp M, Verstraete F, Martin-Delgado M A and Cirac J I 2005 *Phys. Rev. A* **71** 042306
- [64] Murao M, Jonathan D, Plenio M B and Vedral V 1999 *Phys. Rev. A* **59** 156
- [65] Wootters W K and Zurek W H 1982 *Nature* **299** 802
- [66] Dieks D 1982 *Phys. Lett. A* **92** 271
- [67] Cerf N J, Ipe A and Rottenberg X 2000 *Phys. Rev. Lett.* **85** 1754
- [68] Cerf N J and Iblisdir S 2000 *Phys. Rev. A* **62** 040301(R)
- [69] Grosshans F and Grangier P 2001 *Phys. Rev. A* **64** 010301(R)
- [70] Cerf N J, Krüger O, Navez P, Werner R F and Wolf M M 2005 *Phys. Rev. Lett.* **95** 070501
- [71] Fiurášek J 2002 *Phys. Rev. A* **66** 012304
- [72] Fiurášek J 2001 *Phys. Rev. Lett.* **86** 4942
- [73] Owari M, Matsumoto K and Murao M 2004 *Phys. Rev. A* **70** 050301(R)